

Kinetics Study of Reduction / Sulfidation of ZnO and Zinc Titanate Powders in a Drop-Tube Furnace

by

Katsuya Ishikawa

Bachelor of Engineering, Chemical Engineering
University of Tokyo (1980)

Master of Engineering, Chemical Engineering
University of Tokyo (1982)

Submitted to the Department of Chemical Engineering
in Partial Fulfillment of the Requirements
for the Degree of

MASTER OF SCIENCE


at the

MASSACHUSETTS INSTITUTE OF TECHNOLOGY


May 1995

© 1995 Massachusetts Institute of Technology
All rights reserved


Signature of Author


Department of Chemical Engineering
May 10, 1995


Certified by


Maria Flytzani-Stephanopoulos
Thesis Supervisor

Certified by


Adel F. Sarofim
Thesis Supervisor

Accepted by


Robert E. Cohen
Chairman, Committee for Graduate Students

Science
MASSACHUSETTS INSTITUTE
OF TECHNOLOGY

JUL 12 1995

LIBRARIES

Kinetics Study of Reduction / Sulfidation of ZnO and Zinc Titanate Powders in a Drop-Tube Furnace

by

Katsuya Ishikawa

Submitted to the Department of Chemical Engineering on May 12, 1995, in partial fulfillment of the requirements for the degree of Master of Science in Chemical Engineering

Abstract

The reaction kinetics of fine particles of zinc oxide and zinc titanate with H₂S were studied using a drop-tube furnace in order to test the potential of the sorbent injection hot-gas desulfurization process. Fine ZnO sorbent particles with diameter smaller than 50 μm were sulfided with H₂S and/or reduced with H₂ in a laminar flow reactor over the temperature range of 620-910 °C. The reacted sorbent particles were separated from gas and size-classified using a cascade impactor and an absolute filter. Sulfidation conversion was measured by thermo-gravimetric analyses and compared for different particle sizes and reaction conditions. Other sorbents such as zinc titanate, metallic zinc, and ZnO with different porosity were also tested and compared. In the experiments of the reduction of ZnO without H₂S, it was deduced from the change of size distribution of particles that a significant amount of Zn was formed and vaporized. On the other hand, the presence of H₂S suppressed the change of size distribution of particles. This suggests that H₂S suppresses the reduction of ZnO by rapid surface sulfidation and/or that gaseous Zn reacts with H₂S immediately and forms fine particles of ZnS, most of which deposit onto the original particle surface. Formation and vaporization of elemental Zn from zinc titanate sorbents was slower than from zinc oxide with and without H₂S. Surface reaction rate of ZnO and zinc titanate sulfidation was obtained and a reaction model for a single particle was formulated and compared with experimental results in the drop-tube furnace.

Thesis Supervisors : Professor Maria Flytzani-Stephanopoulos
 Professor Adel F. Sarofim

Acknowledgement

This research was supported by CeraMem Corporation.

I would like to thank Prof. Adel F. Sarofim, Prof. Maria Flytzani-Stephanopoulos, and all the members of the catalysis group at the Department of Chemical Engineering, Massachusetts Institute of Technology for their instructive suggestions to this research. Particularly, I owe very much to Dr. Charlie Krueger for his experimental support and suggestions.

I also thank Mr. Tony Modestino for setting up of the drop-tube furnace assembly and instruction of porosimetry measurement.

Finally, I would like to express my thanks to KAWASAKI HEAVY INDUSTRIES Co. LTD. for sending me to M.I.T. and supporting my study here.

Table of Contents

Abstract.....	2
Acknowledgement.....	3
Table of Contents	4
List of Tables	7
List of Figures	8
1. INTRODUCTION	10
1.1 Coal Gasification for Power Generation	10
1.2 H ₂ S Removal	10
1.3 Concept of the Sorbent Injection Process for Hot Gas Cleanup	13
1.4 Thesis Objectives	15
2. PREPARATION OF ZnO SORBENTS	16
2.1 Introduction	16
2.2 Experimental Methods	17
2.2.1 Preparation of Sorbents	17
2.2.2 Physical Analyses	17
2.2.3 Chemical Analyses	21
3. DROP-TUBE EXPERIMENTS	22
3.1 Introduction	22
3.2 Experimental Methods	24
3.2.1 Drop-Tube Experiments	24
3.2.2 Measurement of Sulfidation Conversion by Thermogravimetric Analysis	32
3.3 Description of the Drop-Tube Furnace Assembly	34
3.3.1 Powder Feeder	34

3.3.2	Temperature Profile in the Reactor	35
3.3.3	Mixing of Gas and Sorbent in the Reactor	38
3.4	Presentation and Discussion of	
	Reduction/Sulfidation of ZnO	40
3.4.1	Conditions and Results of	
	Reduction/Sulfidation Experiments	40
3.4.2	Size Distribution of Sorbents After Reactions	42
3.4.3	Effect of Gas Composition and Carrier Gas	45
3.4.4	Effect of the Length of the Reaction Zone	48
3.4.5	Effect of Temperature	48
3.4.6	Particle Size Dependence	52
3.5	Comparison of Different Sorbents	52
3.5.1	Test Results	54
3.5.2	Comparison of ZnO and Zinc Titanate Sorbents	54
3.6	Conclusions	56
4.	MODELING OF SULFIDATION	57
4.1	Introduction	57
4.2	Modeling of Mixing in the Drop-Tube Furnace	58
4.2.1	The Concentration Distribution of	
	H ₂ S in the Reaction Zone	58
4.2.2	The Velocity of Sorbent Particles in	
	the Reaction Zone	61
4.2.3	Summary of the Mixing Model in	
	the Drop-Tube Furnace	63
4.3	Modeling of the Gas-Solid Sulfidation Reaction	65
4.3.1	Introduction	65
4.3.2	Surface Reaction Limitation Model	65
4.3.3	Simple Grain Model	69
4.4	Comparison of Models and Experimental Results	70
4.4.1	Comparison of Grain and Reaction Limiting Model	70
4.4.2	Comparison of Models and Experimental Results	70

4.5 Conclusions	75
5. CONCLUSIONS AND RECOMMENDATIONS	76
5.1 Conclusions	76
5.2 Recommendations	77
6. REFERENCES	78

List of Tables

Table 3.1	List of Experimental Conditions and 41
	Sulfidation Conversions
Table 3.2	Actination Energy of ZnO-2 Sulfidation 53
Table 3.3	Sulfidation Conversions of ZnO and 55
	Zinc Titanate Sorbents
Table 4.1	Binary Diffusion Coefficients of Gas Components 58

List of Figures

Figure 1.1	Equilibrium Concentrations of H ₂ S	12
Figure 1.2	Process Schematic of the Sorbent Injection Process	14
Figure 2.1	Pore Size Distribution of ZnO-2 Sorbent	18
Figure 2.2	Pore Size Distribution of	19
	ZnO (Johnson Matthey) Sorbent	
Figure 2.3	Pore Size Distribution of	20
	ZnTiO ₃ (Pfaltz & Bauer) Sorbent	
Figure 3.1	An Anticipated Reaction Scheme of	23
	ZnO Sulfidation Reaction	
Figure 3.2	Schematic Flowsheet of the Drop-Tube	25
	Furnace Assembly	
Figure 3.3	Powder Feeder Assembly	26
Figure 3.4	Drop-Tube Furnace Reactor Configuration	28
Figure 3.5	University of Washington Mark 3 Cascade Impactor	29
Figure 3.6	Aerodynamic Cut Diameters of	31
	Mark 3 Cascade Impactor	
Figure 3.7	Schematic of the Thermogravimetric Analyzer (TGA)	33
Figure 3.8	Temperature Profiles in the Drop-Tube Reactor	36
	(with different positions of the collection probe)	
Figure 3.9	Temperature Profiles in the Drop-Tube Reactor	37
	(with different set temperatures of the furnace)	
Figure 3.10	Temperature Profiles in the Drop-Tube Reactor	39
	(with different probe positions and gas flow rates)	
Figure 3.11	Particle Size Distributions of Reacted ZnO-2 Sorbent	43
Figure 3.12	Particle Size Distributions of Reacted Metallic ZnO	44
Figure 3.13	Sulfidation Conversions of ZnO-2 Sorbent	46

Figure 3.14	Sulfidation Conversions of ZnO-2 Sorbent with Different Reaction Zone Length	49
Figure 3.15	Arrhenius Plot of ZnO-2 Sulfidation (Sorbent Carrier : CO₂)	50
Figure 3.16	Arrhenius Plot of ZnO-2 Sulfidation (Sorbent Carrier : H₂)	51
Figure 4.1	Mixing Model of the Drop-Tube Reactor	59
Figure 4.2	“k” vs. Retention Time	64
Figure 4.3	Distribution of H₂S Concentration and Particle Velocity in the Reaction Zone	65
Figure 4.4	Schematic Representations of the Reacting Porous Solid by a) Random Pore, b) Simple Grain, and c) random Grain Models	66
Figure 4.5	Conversion Curves by Reaction Models (0.4% H₂S, 750°C)	71
Figure 4.6	Conversion Curves by Reaction Models (1.0% H₂S, 750°C)	72
Figure 4.5	Conversion Curves Test Results vs. Reaction Models (0.4% H₂S, 750°C)	73

CHAPTER 1

INTRODUCTION

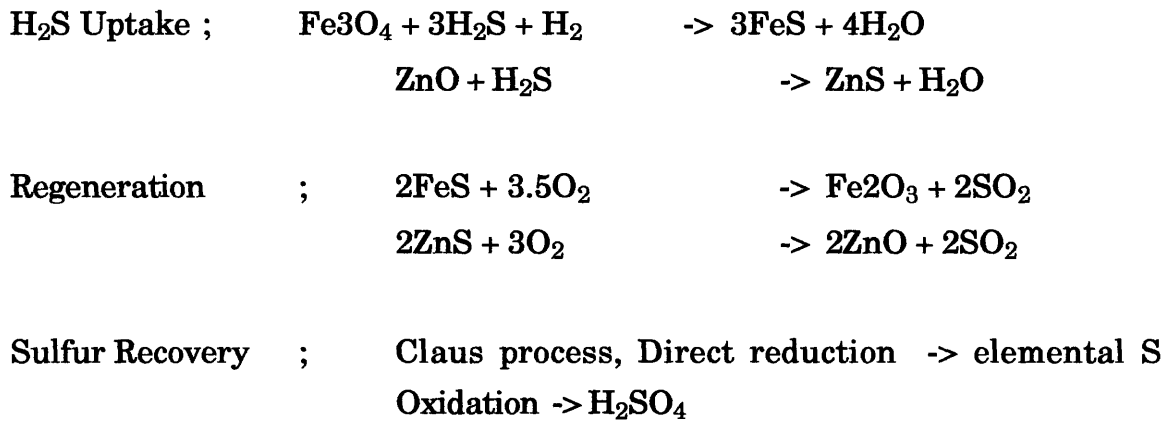
1.1 Coal Gasification for Power Generation

The integrated coal gasification combined-cycle power generation (IGCC) and the gasification-molten carbonate fuel cell (MCFC) system are expected to be more efficient and cleaner alternatives to the conventional pulverized coal fired power plants. For IGCC, efficiencies of 41-44%, much higher than 30-35% of the conventional coal fired power plants, and emission levels of SO₂, NO_x, and CO₂ which satisfy the more stringent environmental standards for new power sources are expected (DOE, 1993). However, to the high efficiency and low emission levels, an advanced gas cleanup process, i.e. hot gas desulfurization and dust removal, are required. For IGCC, H₂S in the coal derived gas should be reduced to less than 100 ppm (97~99% removal) to meet the emission standards of the future, and for CG + MCFC system, H₂S should be even less than 1 ppm (99.97~ 99.99% removal) for preventing contamination and degradation of the fuel cell materials.

1.2 H₂S Removal

Most of sulfur contained in the coal derived gas is known to be in the form of hydrogen sulfide (H₂S). For the removal of H₂S from hot coal derived gas, many metal oxides such as Fe₂O₃, ZnO, CaO, CaCO₃, CuO, MnO, ZnFe₂O₄, 2ZnO-TiO₂, etc. have been studied as sorbents which react with H₂S

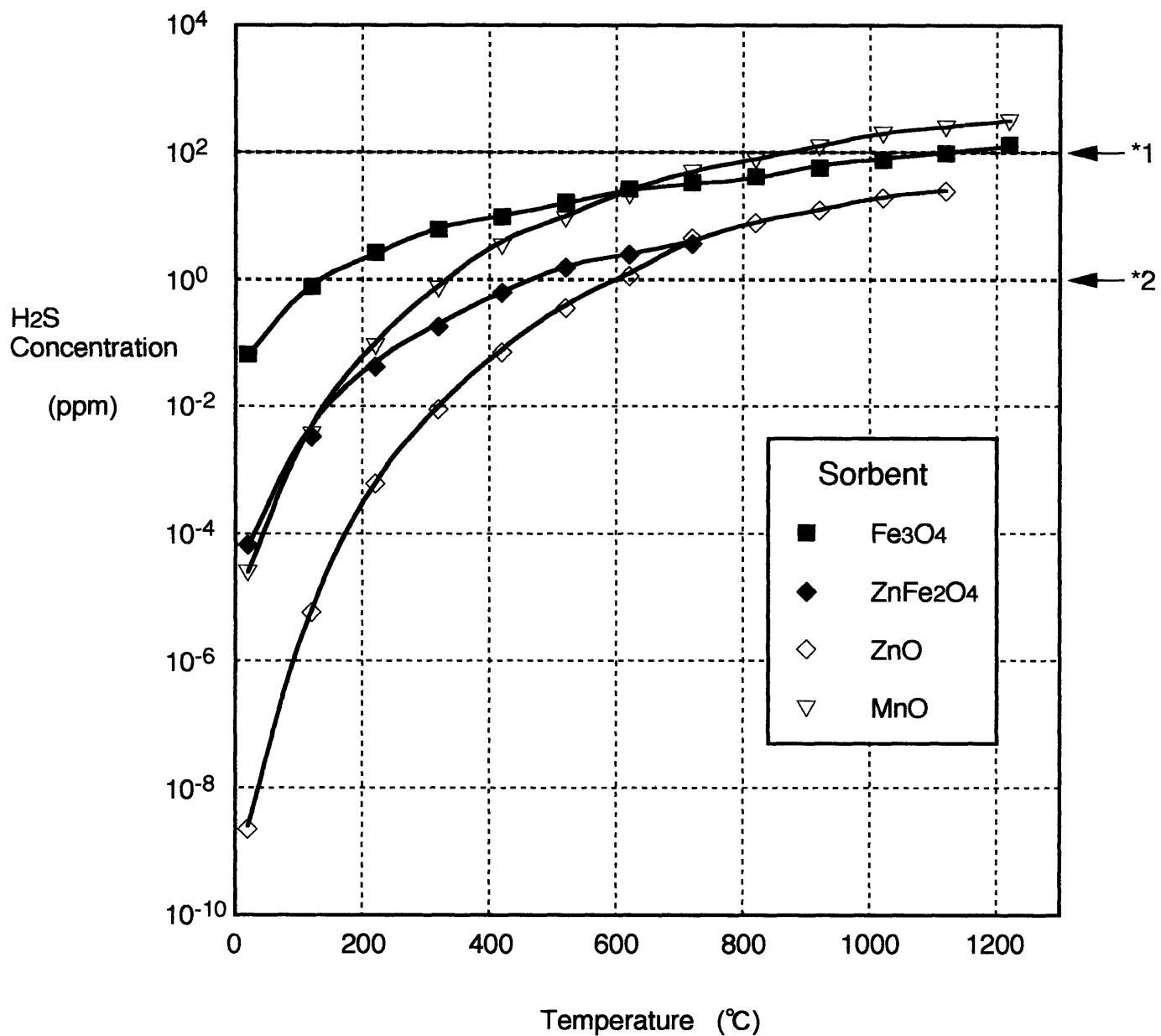
to form solid metal sulfides. Figure 1.1 shows the equilibrium concentrations of H₂S in the hot coal derived gas with some of metal oxides (Ishikawa et al., 1993). The reaction schemes of Fe₂O₃ and ZnO sorbents are as follows;



Some previous studies have investigated the performance of Fe₂O₃ as H₂S sorbent (Hasatani et al., 1980, 1982, 1989; Ishikawa et al., 1993). It was found that Fe₂O₃ was a potential sorbent with high sulfur loading capacity and easiness of regeneration. However, because the equilibrium concentration of H₂S is relatively high, Fe₂O₃ is not suitable for the use above 600°C, especially in high moisture gas.

ZnO has also been studied intensively as a sorbent of H₂S (Flytzani-Stephanopoulos et al., 1985). It was found that ZnO was a potential candidate as a sorbent material with a quite favorable thermodynamic equilibrium of sulfidation with H₂S which enables the removal of H₂S to several ppm even above 600°C. One major problem with ZnO is formation and vaporization of metallic Zn with reduction reaction with H₂ and CO in the coal derived gas. Because of this phenomenon, practical use of ZnO is also limited up to 600°C. Another drawback of ZnO sorbent is the formation of stable sulfate during the regeneration process.

More recently, some mixed oxide sorbents such as Zn-Fe-O and Zn-Ti-O



Gas Composition : H₂ 12 vol%, H₂O 3 vol%

*1 : Tolerant level for IGCC system

*2 : Tolerant level for Coal Gasification + MFCF system

Figure 1.1 Equilibrium Concentrations of H₂S

have been studied as H₂S sorbent to improve the properties of single oxide sorbents (Lew et al., 1989, 1992; Flytzani-Stephanopoulos et al., 1985, 1987). Among the mixed oxides, Zn-Ti-O is now considered one of the most promising sorbent material with high desulfurization performance, easiness of regeneration, and high stability. However, loss of Zn has not been completely prevented yet and long time stability and mechanical durability of the sorbent material in any type of reactor are still a problem.

There are several possible types of reactors, such as moving bed (granular sorbent), fluidized bed (powder sorbent), and fixed bed (particle or honeycomb monolith). Loss of Zn is a common problem to all of these reactors and attrition of the sorbent is to the former two reactors.

1.3 Concept of Sorbent Injection Process for Hot Gas Cleanup

One possible way to avoid all the problems with H₂S sorbents mentioned in the previous section is the sorbent injection process. Figure 1.2 shows the process schematic of the sorbent injection process. In this process, fine powder of the sorbent is injected into the reaction section, actually a gas pipe, and entrained with the coal derived gas. The sorbent is then captured by a porous ceramic micro filter, on which desulfurization reaction still takes place. The filter is back-washed intermittently, and the sorbent removed from the filter is entrained and regenerated by regeneration (oxidizing) gas and sent to another ceramic filter.

Sorbent injection process in conjunction with a porous ceramic micro filter which can collect particles as small as less than 1 micron in diameter may be a solution to many of the problems with Zn sorbent because,

- 1) Sorbent injection process can collect fine particles of zinc sulfide formed with gaseous reaction of Zn vapor and H₂S, thus avoiding the loss of Zn,
- 2) Fine powder reacts with H₂S in duct --> no attrition problem, and

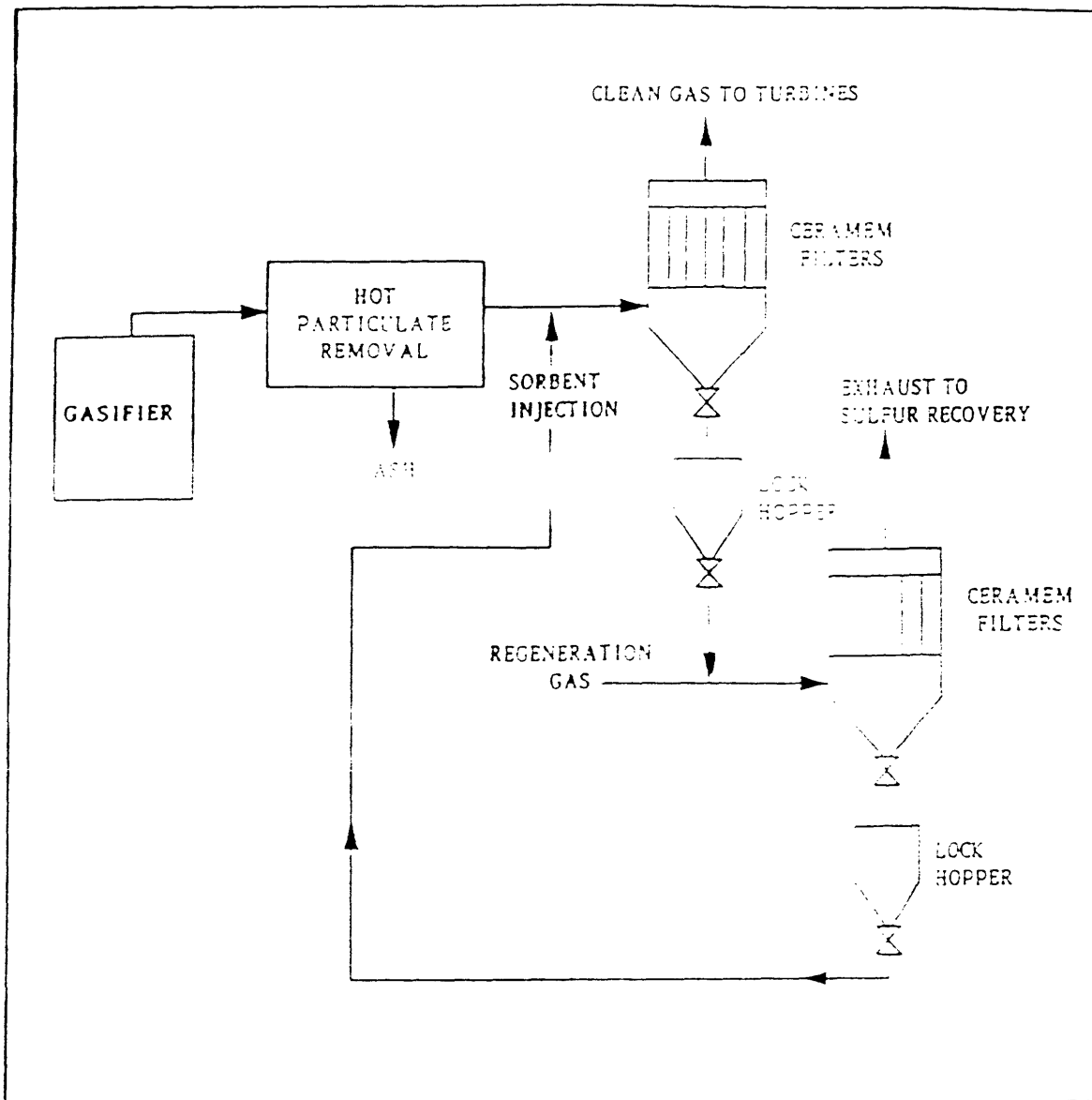


Figure 1.2 Process Schematic of the Sorbent Injection Process
 (Source : CeraMem Corporation)

3) Very fine particle size of the sorbent and the possible pathway of gaseous reaction between H_2S and Zn vapor may enhance the total desulfurization reactivity.

Sorbent injection process can also be a much simpler hot gas desulfurization process than others.

1.4 Thesis Objectives

- 1) Analysis of solid phase reaction characteristics which enables the basic design and evaluation of the potential of sorbent injection hot gas desulfurization process.
- 2) Kinetics evaluation and modeling of the gas-solid sulfidation reaction.
- 3) Comparison of ZnO and Zn-Ti sorbents.

CHAPTER 2

PREPARATION OF ZnO SORBENT

2.1 Introduction

As mentioned in the previous chapter, in the sorbent injection process, many of the requirements in the properties of sorbent material could be much less stringent than other processes. Surface area may be one of these properties. In the conventional processes of advanced gas cleanup, the size and the shape of sorbent depend on the type of the reactor, and the sorbent has to be chemically and thermally stable. Therefore, in the preparation of sorbent material, it is very important to obtain surface area as large as possible while maintaining its stability and strength. One of the many methods proposed to prepare homogeneous and highly dispersed porous oxides is the complexation method (Marcilly et al., 1970).

In the sorbent injection process, very fine powder of sorbent can be used and the micro structure of the sorbent material is expected not to affect much on its reactivity. One of the objectives of this study is to compare several kinds of sorbents in its reactivity and to determine if low surface area, then cheap, material can be used or not. Therefore, in this study, a ZnO prepared by the complexation method, an established method for sorbent preparation, was used as the standard sorbent and compared with more general commercialized materials, i.e. ZnO obtained from Johnson Matthey and ZnTiO₃ from Pfaltz and Bauer. Because the Johnson Matthey ZnO was originally very fine powder and difficult to be fed with the powder feeder, it was pelletized, calcined at 800°C for 72 h, and then crushed into desirable particle size.

2.2 Experimental Methods

2.2.1 Preparation of Sorbents

ZnO-2 sorbent was prepared by the complexation method with citric acid. Citric acid monohydrate and $\text{Zn}(\text{CH}_3\text{CO}_2)_2 \cdot 2\text{H}_2\text{O}$ (zinc acetate dihydrate) were dissolved in water. One mole of citric acid was used for each gram-equivalent of Zn ion. Liquid was evaporated in a rotary evaporator at 65-75°C under vacuum (26-29 in. Hg), then in a vacuum oven (29 in. Hg) at 70-80°C for 4-6 h. The white amorphous foam formed after the evaporation was then calcined at 500°C for 3 h.

2.2.2 Physical Analysis

The pore size distributions of the sorbents were measured using a Micromeritics Autopore 9200 Mercury Porosimeter. Figures 2.1, 2.2, and 2.3 show the pore size distributions of ZnO-2, ZnO (Johnson Matthey), and ZnTiO_3 (Pfaltz & Bauer) sorbents, respectively.

The surface areas of the sorbents were measured with a Micromeritics Flow Sorb 2300 Bet apparatus using a 30% N_2 - 70% He gas. The results are shown below;

Sorbent	Surface area (m ² /g)
ZnO-2 (M.I.T.)	2.0
ZnO-2 (M.I.T.) sulfided at 750°C, 1% H_2S	2.7
ZnO-2 (M.I.T.) reduced at 750°C, 20% H_2	2.6
ZnO(Johnson Matthey)	0.20
ZnTiO_3 (Pfaltz & Bauer)	0.71

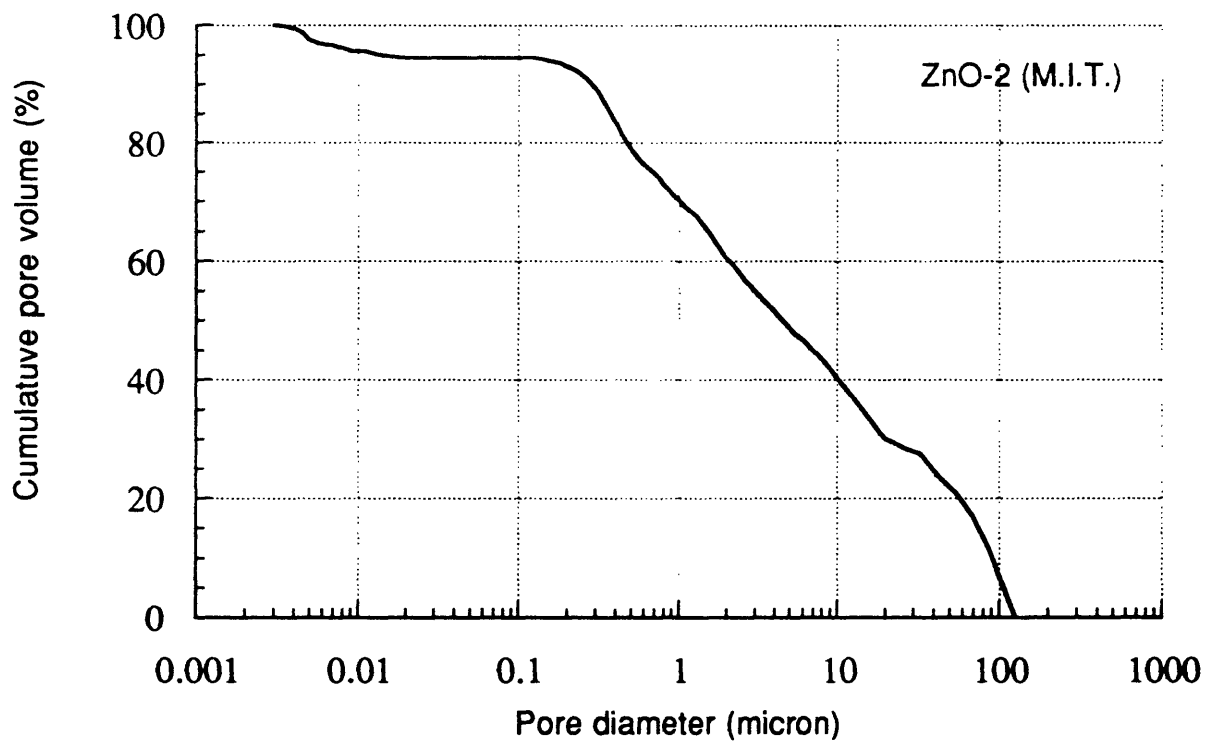


Figure 2.1 Pore Size Distribution of ZnO-2 Sorbent

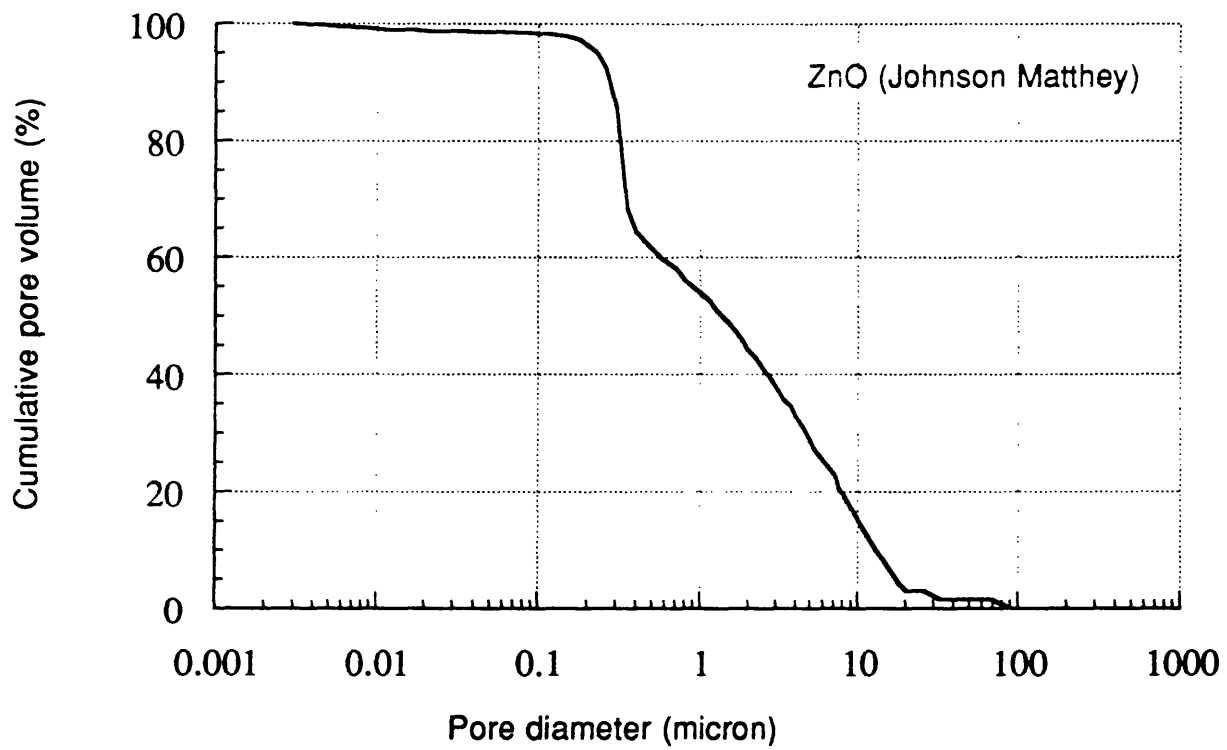


Figure 2.2 Pore Size Distribution of ZnO (Johnson Matthey) Sorbent

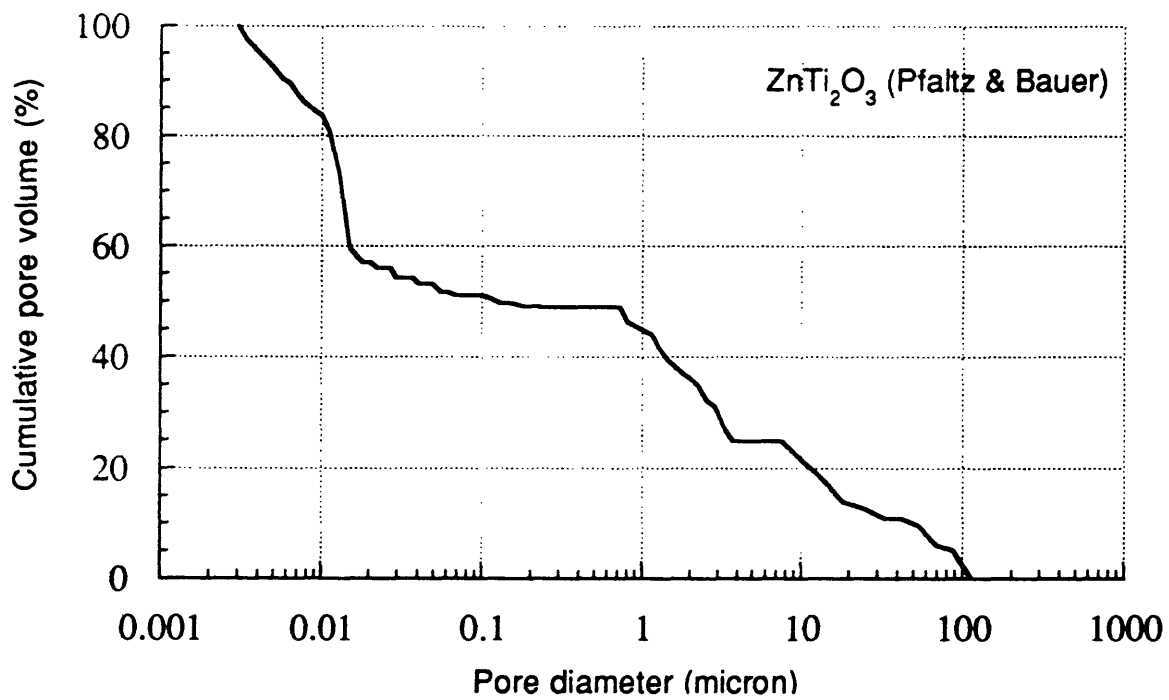


Figure 2.3 Pore Size Distribution of ZnTi₂O₃ (Pfaltz & Bauer) Sorbent

2.2.3 Chemical Analysis

Sulfidation conversion of the reacted ZnO and Zn-Ti sorbents were measured using a Cahn System 113-X thermogravimetric analyzer (TGA). This analysis was based on the weight change with the oxidation of ZnS to ZnO. Schematic of the TGA apparatus and operation procedure are shown in the next chapter.

CHAPTER 3

DROP-TUBE EXPERIMENTS

3.1 Introduction

The purpose of the drop-tube experiment is to obtain reaction kinetics data of ZnO and zinc titanate sulfidation. Figure 3.1 shows an anticipated reaction scheme which includes two reaction pathways, i.e. a solid-gas reaction between ZnO and H₂S, and a gas phase reaction between Zn vapor and H₂S. The effect of the latter reaction path to enhance the total reaction rate was suggested in a previous study (Lew et al. 1990), but its contribution has not yet been studied quantitatively.

The drop-tube furnace was originally designed for the investigation of the combustion mechanism of coal or char particles. Particles and reactant gas are fed into the reactor separately and mixed at the reaction temperature. The sorbent reacts in excess reactant in the gas, so the gas composition can be assumed to be constant. The mixed gas is quenched immediately by a water-cooled probe inserted into the reactor from the bottom so that the reaction is “frozen” after a certain contact time.

By using a drop-tube reactor in conjunction with a cascade impactor, sulfidation conversion of different size sorbent particles can be measured separately because the cascade impactor size-classifies the particles in the reacted gas flow. Furthermore, the change of size distribution of the sorbent after the reaction could provide information on the reduction of ZnO and

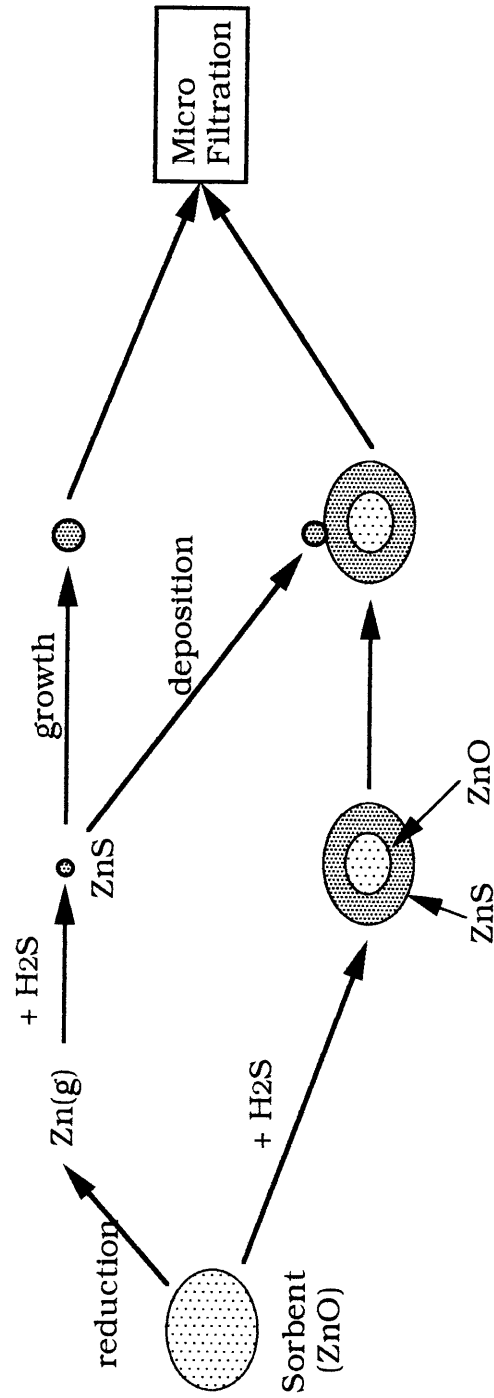


Figure 3.1 An Anticipated Reaction Scheme of ZnO Sulfidation Reaction

vaporization of Zn as shown in the following sections.

3.2 Experimental Methods

3.2.1 Drop-Tube Experiments

Figure 3.2 shows the flow schematic of the drop-tube test facility. Sorbent particles were previously classified in a known size range and fed into a drop-tube down-flow reactor by one of the components of a simulated coal gasifier-exit gas, which comprises H_2S , H_2 , CO_2 , and N_2 . Other components contained in the real coal gas such as CO , H_2O , and trace of COS are omitted from the present experiments. Each gas component was fed from a gas cylinder and the flow rate was controlled by a mass flow controller. The sorbent was introduced through a particle feeder and flowed with the other gas components for a certain distance, i.e. a certain contact time. In addition to the reactant gas, N_2 was fed to the water-cooled collection probe for quenching the reacted gas. The reacted gas and N_2 from the collection probe were then led to the cascade impactor, in which sorbent particles contained in the gas flow were classified according to the particle size into seven stages and a final paper filter.

Figure 3.3 shows the powder feeder. Sorbent powder is held in a vial sealed with an O-ring. The vial is supported by the piston of a syringe pump which moves at a slow, constant speed. The carrier gas is fed into the vial and exits through a capillary discharge tube at the top of the powder entraining a small amount of the powder continuously. The whole feeder including the tube between the feeder and the reactor is vibrated by an electric vibrator to keep the feed rate constant and to prevent clogging. The feed rate can be controlled by the speed of the syringe pump movement, but it also depends on the particle size and other characteristics of the powder.

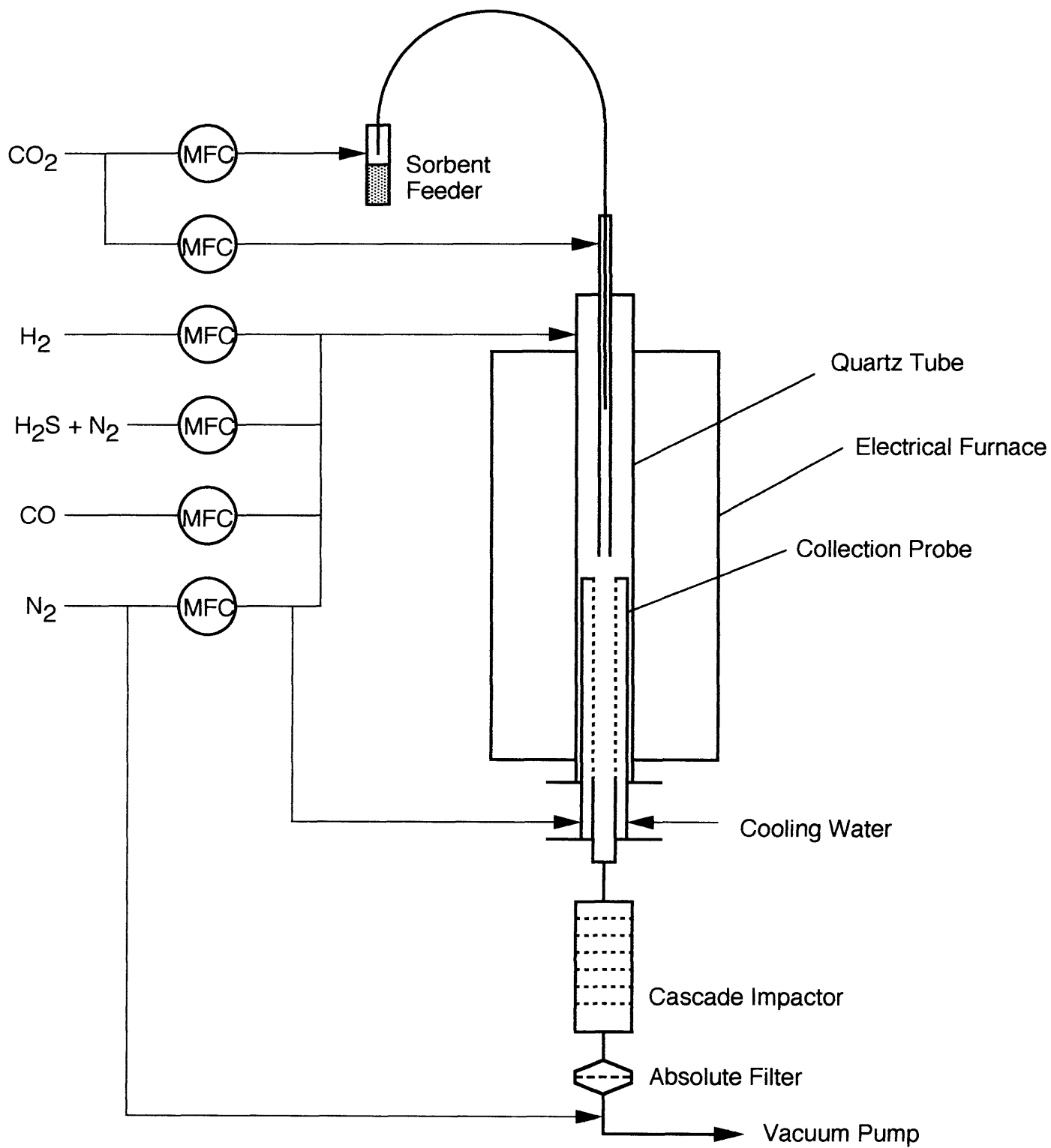


Figure 3.2 Schematic Flowsheet of the Drop-Tube Furnace Assembly

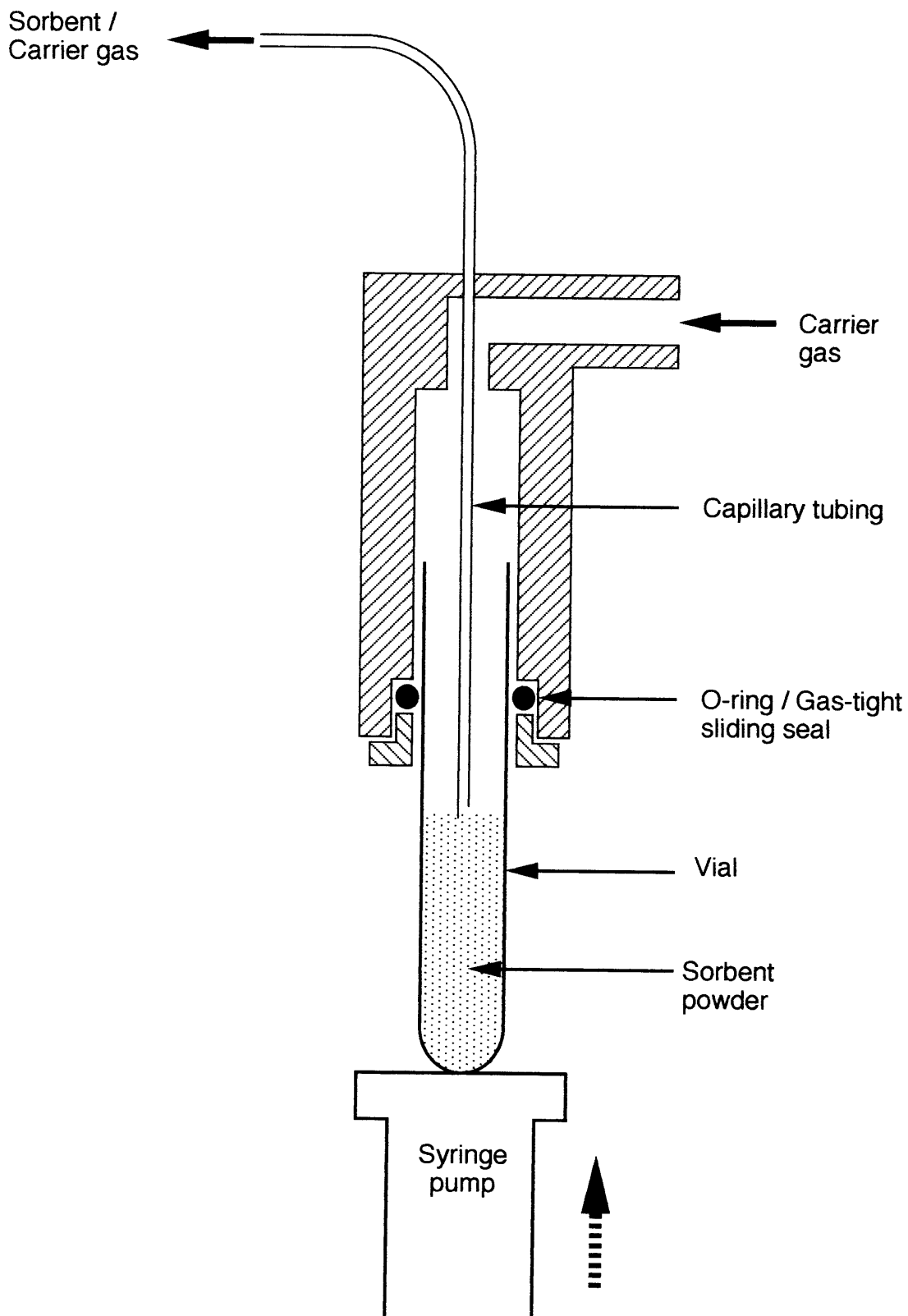


Figure 3.3 Powder Feeder Assembly

Previous size classification of sorbent was done with sieves with the mesh openings of 30, 40, 50, and 63 μm ; however, it was revealed by the size measurement using the cascade impactor that even after cutting the smaller size powder with one of the sieves above, fine powder smaller than 10 μm in diameter still exists. This is because of the limited ability of size separation of dry sieving.

Figure 3.4 shows the electric furnace and reactor configuration. The electric heater has two elements and can heat the reactor up to 950 °C. The reactor is a 1.5 inch I.D. quartz tube and the feeder probe through which the sorbent is entrained by carrier gas is a 1/8 inch O.D. quartz tube. The collection probe is made of stainless steel and cooled by cooling water. The collection probe has a porous inner wall through which N_2 gas was emitted into the reacted gas for quenching. The position of the feeder probe and the collection probe can be changed independently so that the position and the length of the reaction zone can be changed freely. Sorbent powder was entrained by one of the gas components, usually CO_2 , and mixed with the other components in the reaction zone. The velocity of the gas flow containing the sorbent (“jet flow”) is usually about 20 times higher than the other reactant gas flowing outside the feeder probe (“bulk flow”), so the mixing of the “jet” and “bulk” flows was expected to be quite rapid. If this was the case, gas composition in the reaction zone could be considered constant because the stoichiometric ratio of H_2S and the sorbent was at least four. As shown in the following sections, however, it was revealed that the inlet zone in which the mixing was incomplete was long enough compared to the length of the reaction zone that the effect of mixing on reaction could not be neglected.

Figure 3.5 (Cascade Impactor Instruction Manual) shows the schematic of the University of Washington Mark 3 type cascade impactor, which was used in this study. This cascade impactor has seven stages for size separation. The collection efficiency of each impaction stage is given as,

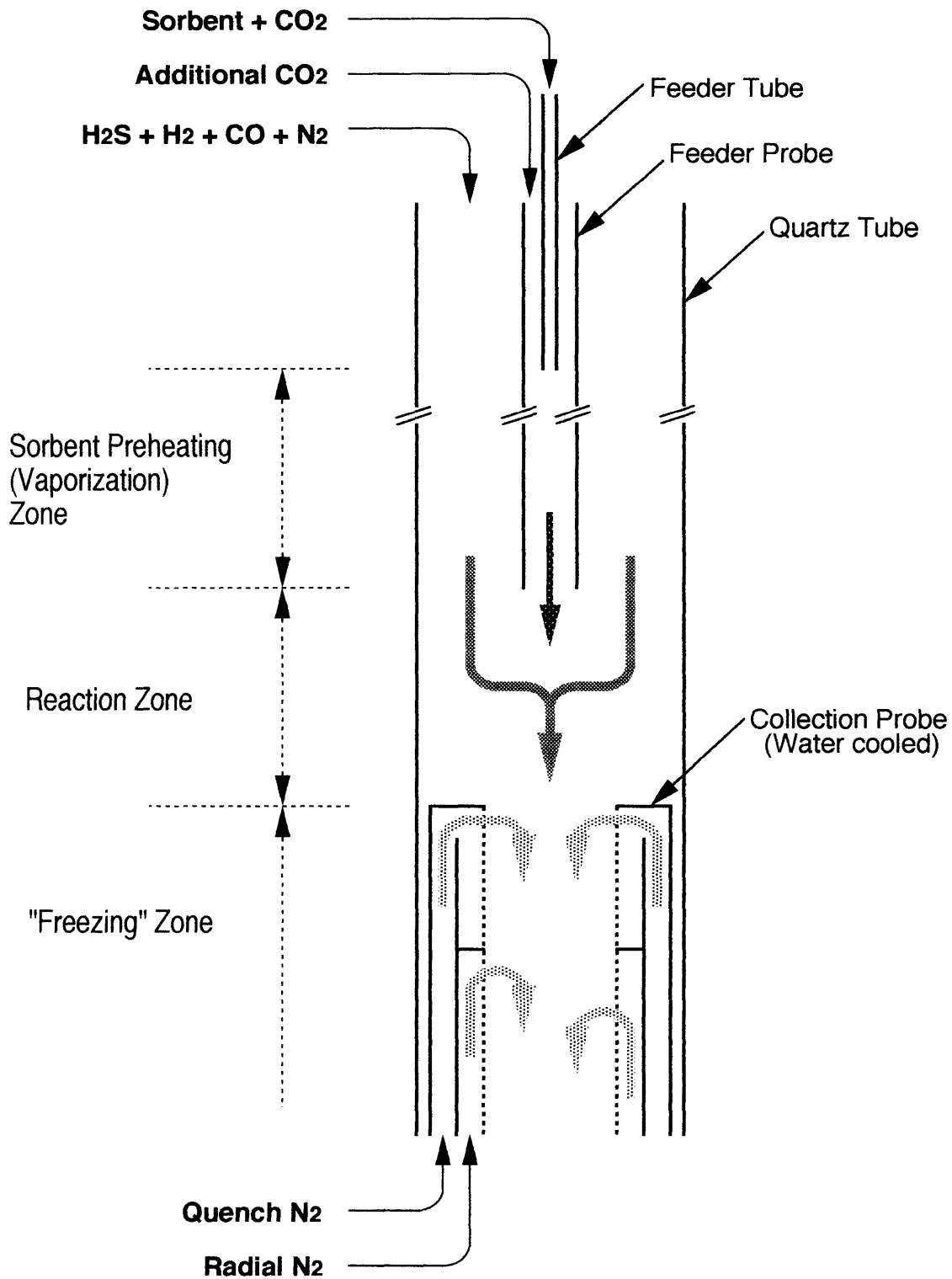


Figure 3.4 Drop-Tube Furnace Reactor Configuration

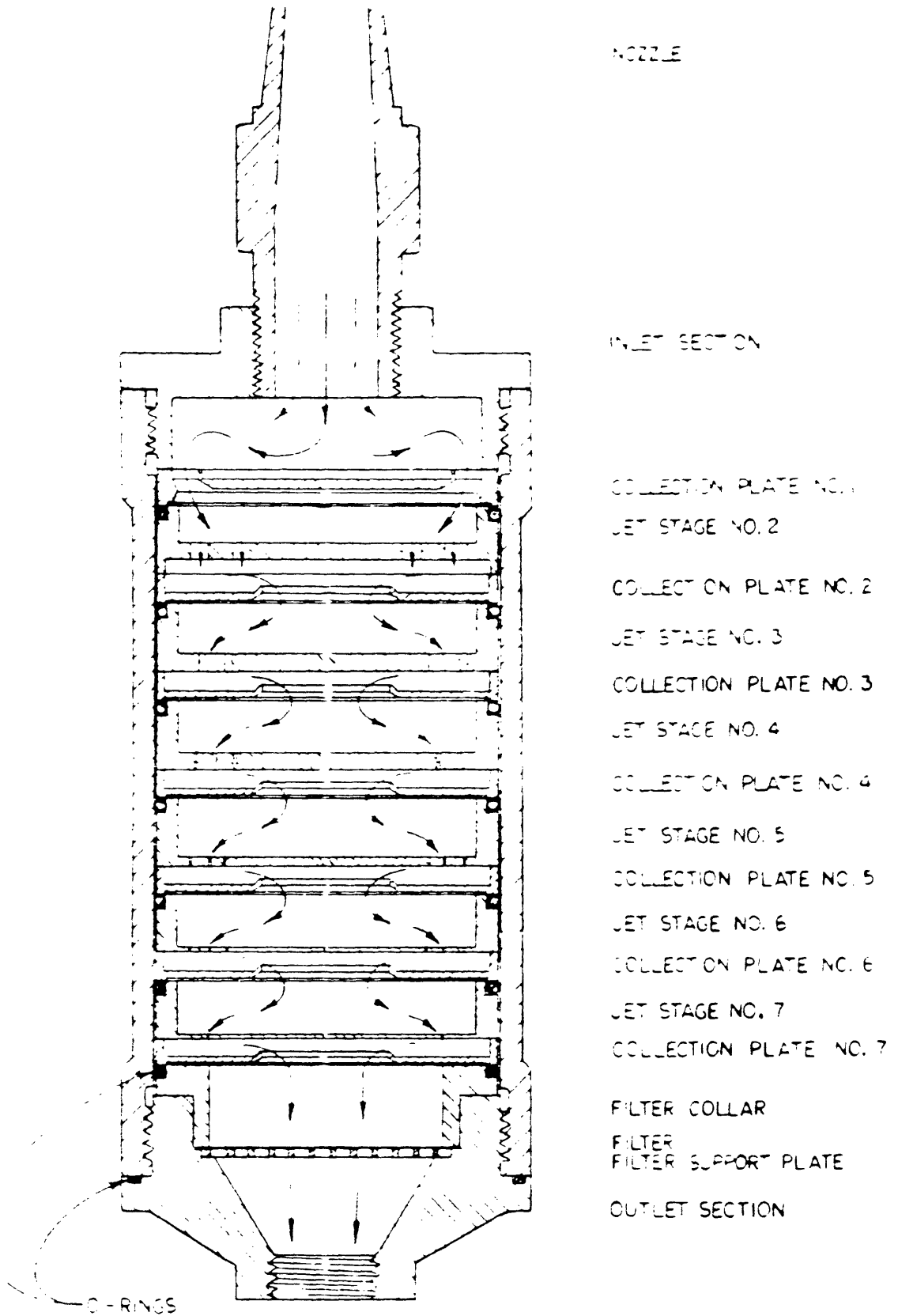


Figure 3.5 University of Washington Mark 3 Cascade Impactor

$$\psi = \frac{\rho v d^2}{\eta W} \times \text{constant} ;$$

ψ : impaction efficiency
 ρ : powder density
 η : fluid viscosity
 v : fluid jet velocity
 d : aerodynamic diameter of powder
 W : jet diameter or width of slit

By changing jet size and jet velocity, each stage has different cutting point in particle size. Figure 3.6 shows a sample separation curve obtained by the same cascade impactor as used here (Cascade Impactor Instruction Manual).

A typical procedure of the drop-tube experiment was as follows.

- 1) Put the sorbent into the sample vial and set up the powder feeder.
- 2) Feed cooling water to the furnace.
- 3) Start heating the furnace (About two hours to the set point).
- 4) At the set temperature, feed cooling N₂ to the collection probe and insert the probe into the reactor.
- 5) Attach the cascade impactor and the filter holder to the gas outlet of the reactor.
- 6) Connect the line from the reactor outlet to the vacuum pump and start the pump immediately. Adjust the opening of the valve before the pump to keep the pressure in the reactor at atmospheric pressure (Because the reactor is not gas-tight, the pressure should be kept at 0 psi to prevent leakage).
- 7) Watching and adjusting the pressure, start feeding the components of the reactant gas except the carrier of the sorbent one by one.
- 8) Turn on the vibrator and the syringe pump of the powder feeder.
- 9) Start feeding the carrier gas. (Beginning of the reaction)
- 10) After 30~60 minutes, stop the reaction in the reverse order of 6) ~ 9).
- 11) Disconnect the cascade impactor and the filter holder.
- 12) Pull out the probe and cool down the furnace.
- 13) Weigh each stage of the cascade impactor to mg and store the captured powder separately.

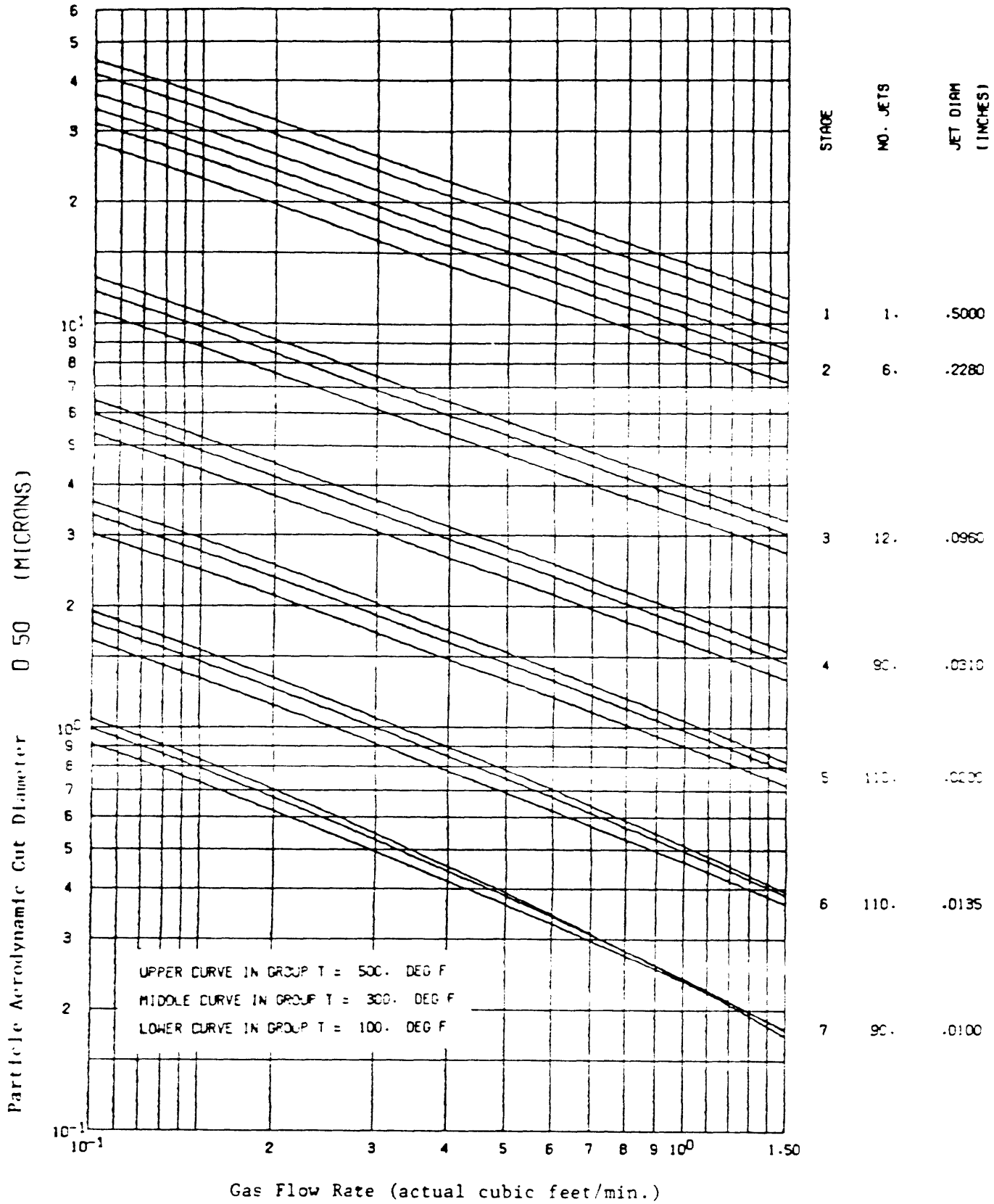
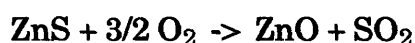


Figure 3.6 Aerodynamic Cut Diameters of Mark 3 Cascade Impactor

3.2.2 Measurement of Sulfidation Conversion by Thermogravimetric Analysis

A Cahn System 113-X thermogravimetric analyzer with a Cahn 2000 electrobalance, a Micricon temperature controller, and a Bascom Turner data acquisition system was used for the measurement of extent of sulfidation of sorbents sulfided in the drop-tube furnace assembly. To this effect an oxidation experiment, i.e. regeneration of the oxide sorbents was performed in the thermogravimetric analyzer (TGA). Figure 3.7 shows the flow schematic of the TGA. A small amount of sulfided sorbent is held in the sample pan made of quartz and its weight change is detected by the electrobalance, the signal of which is sent to the data acquisition system. The reactant gas, a mixture of O₂ and N₂, flows downward in the reactor tube and reacts with the sorbent in the sample pan.

The sample sorbents were partially sulfided ZnO or zinc titanate. This means that the samples could include not only ZnS but also ZnO, TiO₂, any kind of Zn-Ti mixed oxide, and possibly metallic Zn formed by reduction with H₂ in the reactant gas. The sample might also contain adsorbed H₂S or H₂O. In order to obtain sulfidation conversion by the weight change of the sample with the oxidation reaction of ZnS,



the effect of adsorbed material and metallic Zn had to be subtracted by heating the sample at 750°C in N₂ before introducing O₂.

The procedure of the measurement of sulfidation conversion with TGA is as follows.

1. Put 0.005~0.02g of sample in the quartz pan and set up the TGA.
2. Heat up the sample in N₂ flow (400-500 SCCM) from room temperature to 750°C in 1 hour.

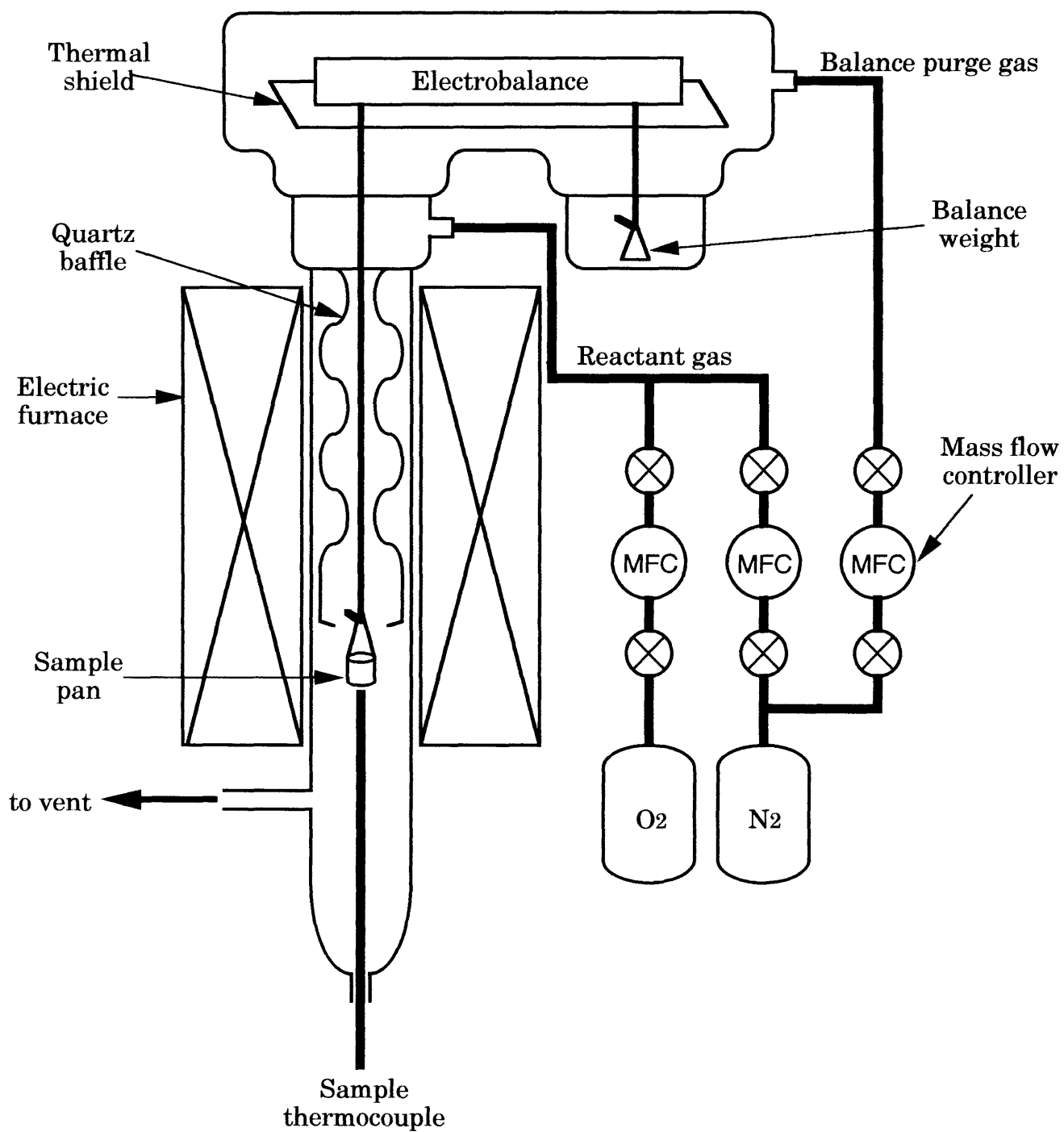


Figure 3.7 Schematic of the Thermogravimetric Analyzer(TGA)

3. After the weight change with heating at 750°C is stabilized, introduce O₂ to a total concentration in the gas flow through the TGA is 6 vol%.
4. Measure the weight change at 750°C.
5. After the weight change is stabilized, stop O₂ and cool down.
6. From the weight difference of the sample between just before the introduction of O₂ and after the reaction, calculate the conversion, X.

$$X = \frac{\text{weight change (g)}}{(\text{mole weight of ZnS} - \text{mole weight of ZnO (g)}) \times (\text{mole \# of Zn in sample})}$$

3.3 Description of the Drop-Tube Furnace Assembly

3.3.1 Powder Feeder

Though the feed rate of sorbent should be controlled by the piston speed of the syringe pump, it was found that the property of the powder and the flow rate of the carrier gas had more dominant effect on the powder feed rate. In other words, the ability of the gas to pick up the powder from the sample tube was limiting the feed rate, and if the piston speed was set over the limit, plugging of the capillary tube occurred immediately because the edge of the tube went down into the powder bed.

For most of the sorbents tested, the limit of the feed rate for stable feeding was around 0.5~1g/hr at the carrier gas flow rate of 120 SCCM and there was almost no problem in feeding unless lower flow rate of the carrier gas was used. In the case of Johnson-Matthey ZnO, stable feeding was very difficult because the powder is originally very fine, mostly under 3μm in diameter. In order to solve this problem, the powder was pelletized at 6000 psi and annealed at 800°C for 72 hr. The pellet was then crushed and sieved before

use in the experiments.

The composition of the carrier gas may also have some effect on feed rate, but the differences among the tested gases, i.e. CO₂, H₂, and H₂S, were found to be negligible.

3.3.2 Temperature Profile in the Reactor

As is usually the case with electric furnaces, the temperature profile in the reactor was not uniform. Also, it had been found in the previous studies that the position of the collection probe had a strong influence on the temperature profile in the reactor because the cooling load of the probe changed with its length inserted into the reactor. In order to determine the appropriate setting for reaction experiments in which the temperature should be as uniform as possible, temperature profiles at various conditions were measured.

Figure 3.8 shows temperature profiles with different positions of the collection probe. It was found that the higher the probe position, the higher the peak temperature was at the same setting temperature of the furnace. This is because as the length of the probe inserted in the furnace becomes longer, the cooling load increases, then the output of the electric heater increases. In all cases, the temperature difference between the peak point and just above the collection probe was 100°C or more. However, when the position of the probe was higher up in the tube, the temperature gradient above the probe became steeper, in other words, the region with temperature gradient became smaller. With this reason, most of the drop-tube experiments were done with the collection probe at 16" from the top of the furnace, the highest position possible for probe insertion from the bottom of the tube.

Figure 3.9 shows temperature profiles with different set temperatures of the furnace with the collection probe at 16" from the top of the furnace. The

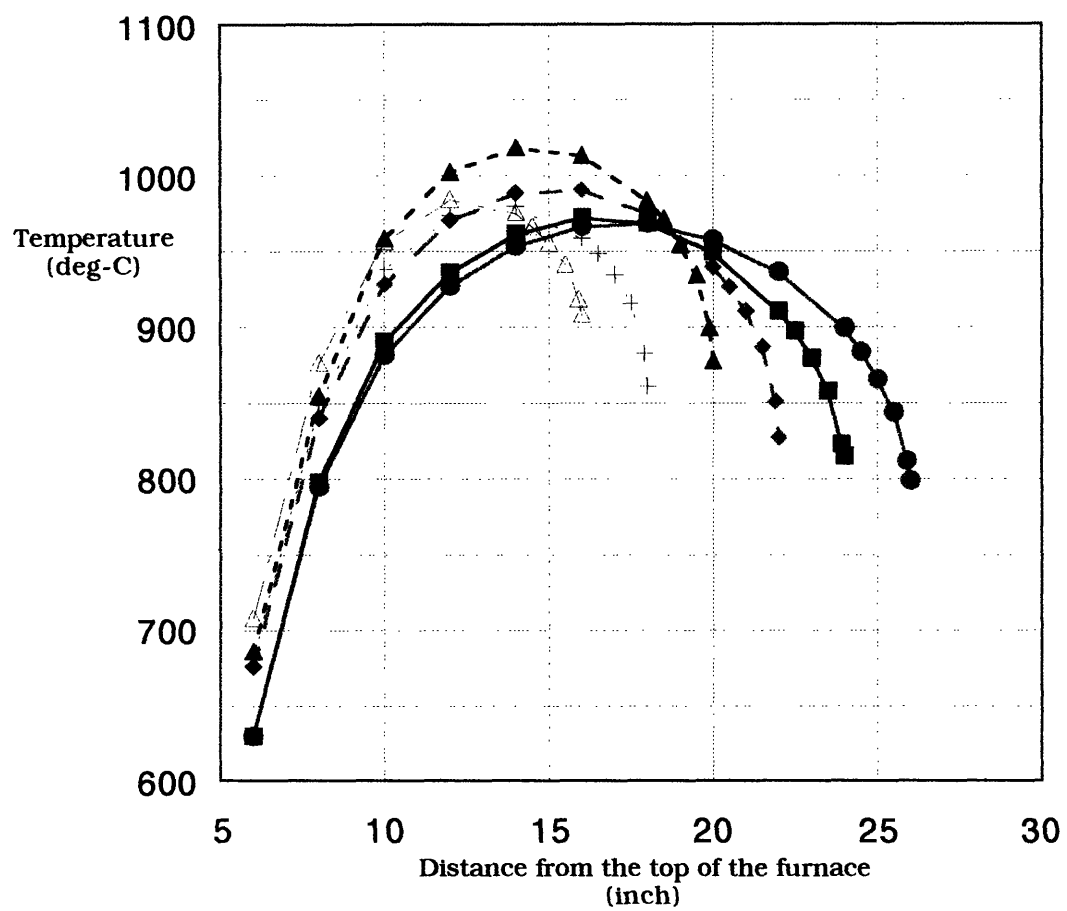


**Figure 3.8 Temperature Profiles in the Drop-tube Reactors
(with different positions of the collection probe)**

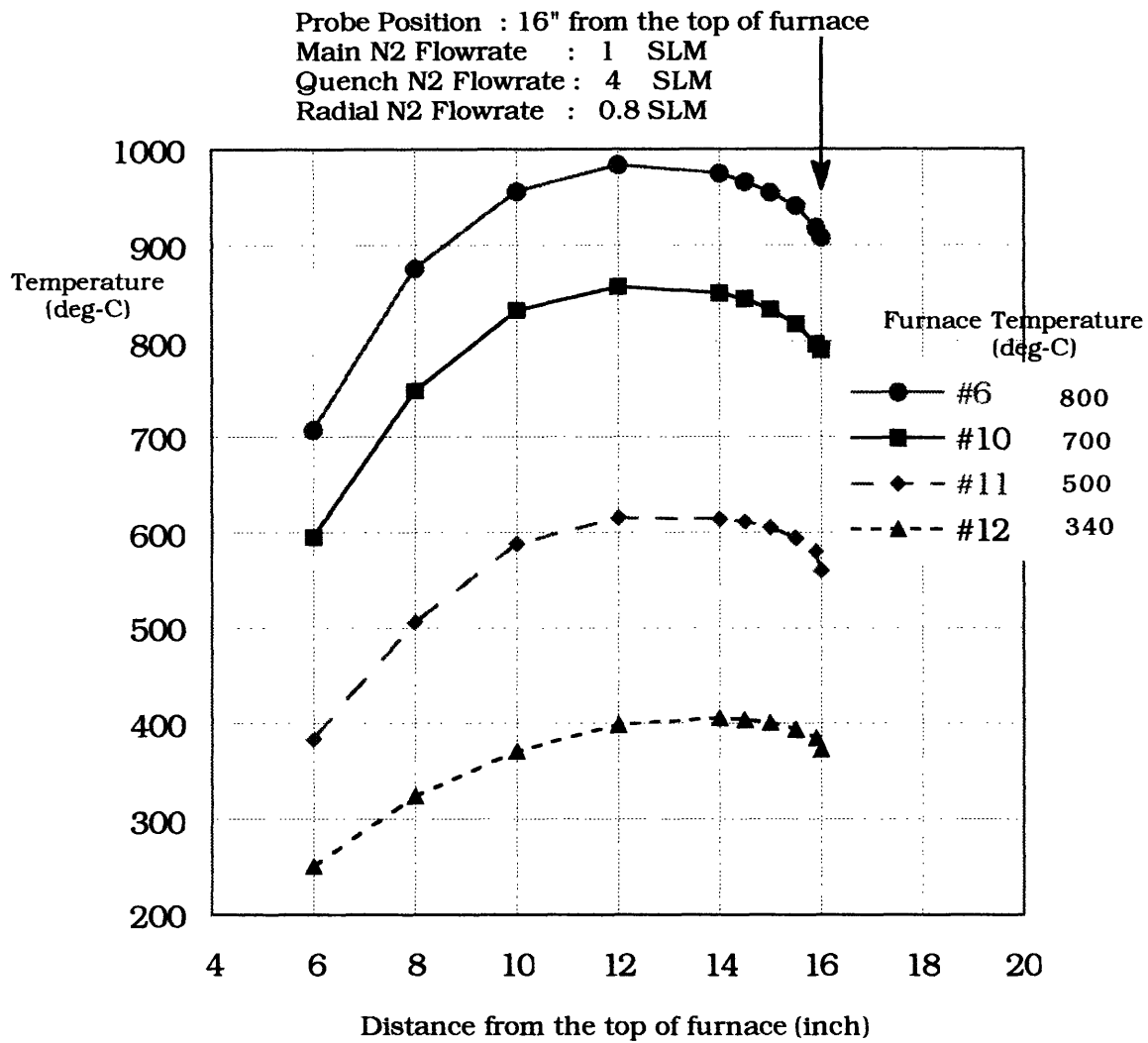


Figure 3.9 Temperature Profiles in the Drop-tube Reactor (with different set temperatures of the furnace)

temperature gradient was smaller at lower set points, but the position of the peak point did not differ much. Furnace set point at 600°C was selected as the standard experimental condition. With this setting, the peak temperature was about 750°C and in the region between 6” and 1” from the top of the collection probe could be considered isothermal with the temperature difference less than 15°C. Therefore, the reactor could be assumed to be isothermal at the average temperature.

Figure 3.10 shows the effect of gas flow in the reactor on the temperature profiles with the collection probe at 26” and 28” from the top of the furnace. In both cases, the effect of gas flow was negligible.

3.3.3 Mixing of Gas and Sorbent in the Reactor

In addition to the temperature gradient, there are other deviations from the ideal, isothermal laminar flow reactor, that is, the gradient of gas composition in the reaction zone and nonuniformity of the velocity of sorbent powder.

As the reaction zone begins at the point where the “jet” blows into the “bulk flow”, the existence of insufficient mixing region (“inlet region”) at the top of the reaction zone is inevitable. In the inlet region, gas composition surrounding sorbent particles and the velocity of the particles change gradually from the values in the jet flow to that in the bulk flow. The problem is the length of the inlet region relative to the whole reaction zone. If the length of the inlet region is sufficiently small, say less than 1/10 of the length of the reaction zone, the ideal reactor model may be applied. Otherwise, the existence of gas composition and particle velocity gradients should be considered in the reactor model.

As shown in the following sections, some of the reaction experiments were done to determine the extent of the mixing effect by changing carrier gas,

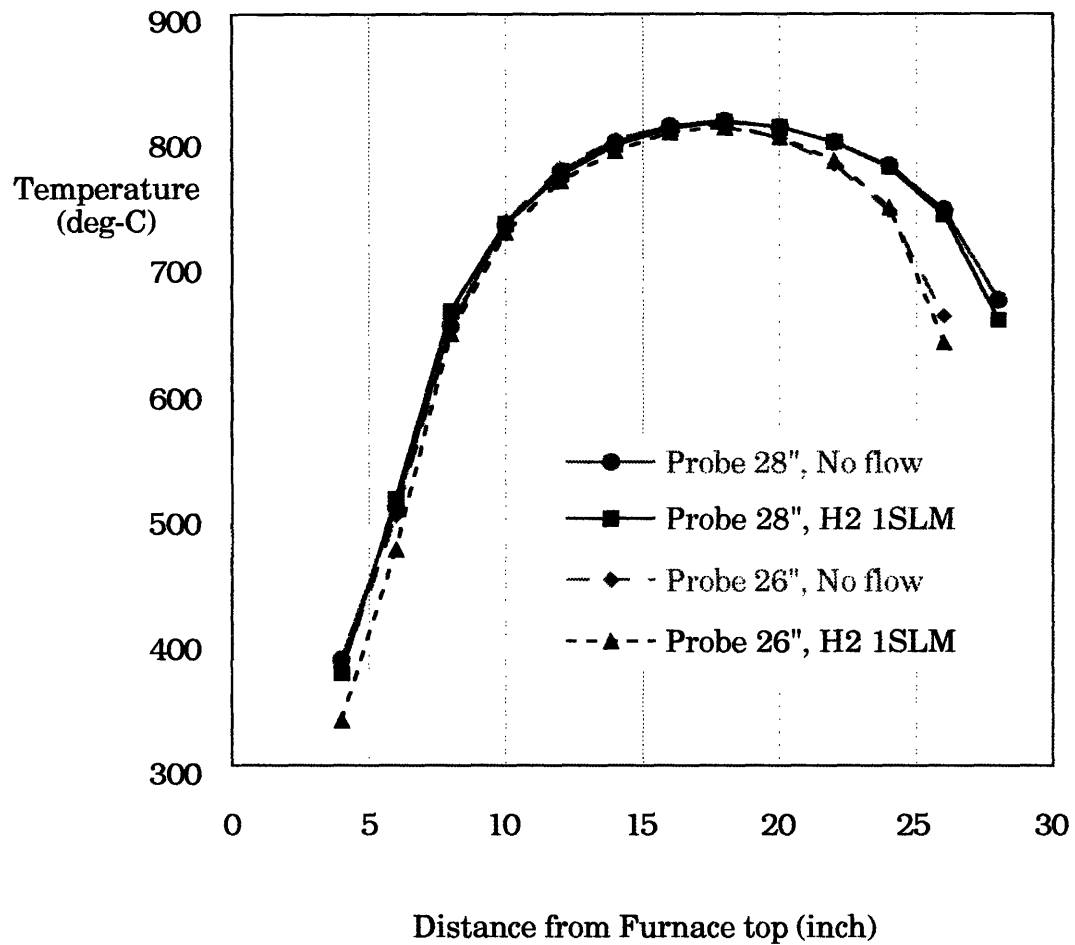


Figure 3.10 Temperature Profiles in the Drop-tube Reactor (with different probe positions and gas flow rates)

jet flow rate, or bulk flow rate. From the results of those experiments, a mixing model in the drop-tube reactor was examined.

3.4 Presentation and Discussion of Reduction/Sulfidation Results of ZnO

3.4.1 Conditions and Results of Reduction/Sulfidation Experiments

The reduction (no H₂S in the reactant gas) and sulfidation (with H₂S) experiments of three kinds of sorbents were done in various conditions. The following is the range of test conditions of most experiments.

Sorbent : **ZnO-2(M.I.T.)**
 ZnO(Johnson Matthey)
 ZnTiO₃(Pfaltz & Bauer)

Sorbent Size : 30 ~ 63 μm (dry sieving)

Temperature : 620, **750**(standard), 850 °C

Reaction Zone : 5, **10**(standard), 30 cm

Bulk Flow Velocity: **5.0**(standard), 10.0 cm/s

Jet Flow Velocity : 48, **97**(standard) cm/s

Gas Molar Composition :

 H₂S; 0(reduction), 0.4, **1.0**(standard), 2.0, 4.0 %

 H₂; 0, **20**(standard) ~ 40 %

 CO₂; **18** %

Carrier (Jet) Gas : **H2**(standard), CO₂, H₂S 6% - N₂

Experimental conditions and sulfidation conversions of ZnO-2(M.I.T.), ZnO(Johnson Matthey), and ZnTiO₃(Pfaltz & Bauer) sorbents are summarized in Table 3.1. In the measurement of sulfidation conversion by oxidation in the TGA, no weight reduction associated with the vaporization of metallic Zn

Table 3.1 List of Experimental Conditions and Sulfidation Conversions

Sorbent / Gas Flow	Sorbent:	Conditions:	Carrier Gas:	React. zone:	temp(C)	time(sec)	CH2S(%)	Sulfidation conversion (%)					
								CI Stage 1	CI Stage 3	CI Stage 5	CI Stage 3	CI Stage 5	
ZnO-2 / CO2 carrier	ZnO-2(MIT) 30~50micron sieved	620 / 750(standard) / 850 deg C	CO2 or H2 or H2S	2" / 4"(standard) / 12"	620	2	2	1	0.9	0.9	1.1	0.9	1.1
ZnO-2 / CO2 carrier	ZnO(Johnson Matthey) 30~40micron sieved	Jet flow : 97(standard) or 48 cm/s	CO2 or H2 or H2S	2" / 4"(standard) / 12"	620	2	2	2	1.6	1.4	2.1	1.6	2.1
ZnO-2 / CO2 carrier	ZnTiO3(Pfaltz & Bauer) 30~50micron sieved	Bulk flow : 5(standard) or 10 cm/s	CO2 or H2 or H2S	2" / 4"(standard) / 12"	620	2	2	4	2.8	2.3	2.5	2.8	2.5
ZnO-2 / CO2 carrier					750	2	2	1	1.5	1.5	2.4	1.5	2.4
ZnO-2 / CO2 carrier					750	2	2	2	3.3	3.8	4.2	3.3	4.2
ZnO-2 / CO2 carrier					750	2	2	4	3	3.8	1.4	3	1.4
ZnO-2 / CO2 carrier (2" react. zone)					750	1	1	4	0	0	0	0	0
ZnO-2 / CO2 carrier (12" react. zone)					750	6	6	0.4	3.5	5.9	10.2	3.5	10.2
ZnO-2 / CO2 carrier (12" react. zone)					750	6	6	1	7.8	11.7	10	7.8	10
ZnO-2 / CO2 carrier (12" react. zone)					750	6	6	2	8.3	11.7	15.2	8.3	15.2
ZnO-2 / CO2 carrier (No H2)					750	2	2	1	0.8	0.8	0.74	0.8	0.74
ZnO-2 / CO2 carrier (half jet flow)					750	2	2	1.1	3.8	4.2	3.9	3.8	3.9
ZnO-2 / 6%H2S carrier					750	2	2	1	8.8	9.5	10.6	8.8	10.6
ZnO-2 / 6%H2S carrier (doubled bulk flow)					750	1	1	0.58	8	8.2	8.9	8	8.9
ZnO-2 / H2 carrier					620	2	2	1		1.65	2.4		2.4
ZnO-2 / H2 carrier					750	2	2	1	4	5.2	6.1	4	6.1
ZnO-2 / H2 carrier					850	2	2	1	6	4.3	4.4	6	4.4
ZnO(Johnson Matthey) / H2 carrier					750	2	2	1	0.12	0.6		0.12	0.6
ZnTiO3 / H2 carrier					750	2	2	1	0.9	1.6		0.9	1.6

during the heating in N_2 was observed. This indicates that if any metallic Zn was deposited on the particles, it was quickly either sulfided by H_2S or oxidized by product water.

3.4.2 Size distributions of sorbent after reactions

Figure 3.11 shows size distributions of ZnO-2 sorbent measured with the cascade impactor after reduction/sulfidation reaction at various conditions. It was clear that the powder over $10\ \mu m$ size decreased while the $1.5\sim 5\ \mu m$ size range increased after reduction. This suggests that formation and vaporization of metallic zinc take place in reduction.

With H_2S in the reactant gas, however, the change of size distribution is small or negligible except at $850^\circ C$. This result coincides with a previous study that H_2S had a suppressive effect on the reduction of ZnO (Lew et. al. 1992). The mechanism of the suppression of fines formation with H_2S may be the suppression of the reduction reaction itself or immediate sulfidation of formed Zn vapor. In order to examine the latter effect of H_2S separately, fine powder of metallic Zn was fed into the reactor with and without H_2S and its particle size distribution was measured. Figure 3.12 shows the size distributions of metallic Zn powder at the outlet of the reactor a) without H_2S at room temperature (i.e. no reaction or vaporization), b) without H_2S at $750^\circ C$ (i.e. no reaction but vaporization), c) with 1 vol% H_2S at $750^\circ C$, d) with 1 vol% H_2S at $850^\circ C$. The gas composition other than H_2S was the same for all the cases, i.e. H_2 20%, CO_2 17%, and N_2 balance and the carrier gas was pure H_2 . The size distributions of case a) and case c) were almost the same, that is, little fine powder was formed with sulfidation at $750^\circ C$. On the other hand, in case b), the change of size distribution by vaporization of Zn at $750^\circ C$ was obvious. While more than 80 wt% of the powder was originally larger than $10\ \mu m$, only 20 wt% remained over $10\ \mu m$ after vaporization at $750^\circ C$. This result shows that the existence of no more than 1 vol% of H_2S inhibited the vaporization of Zn almost

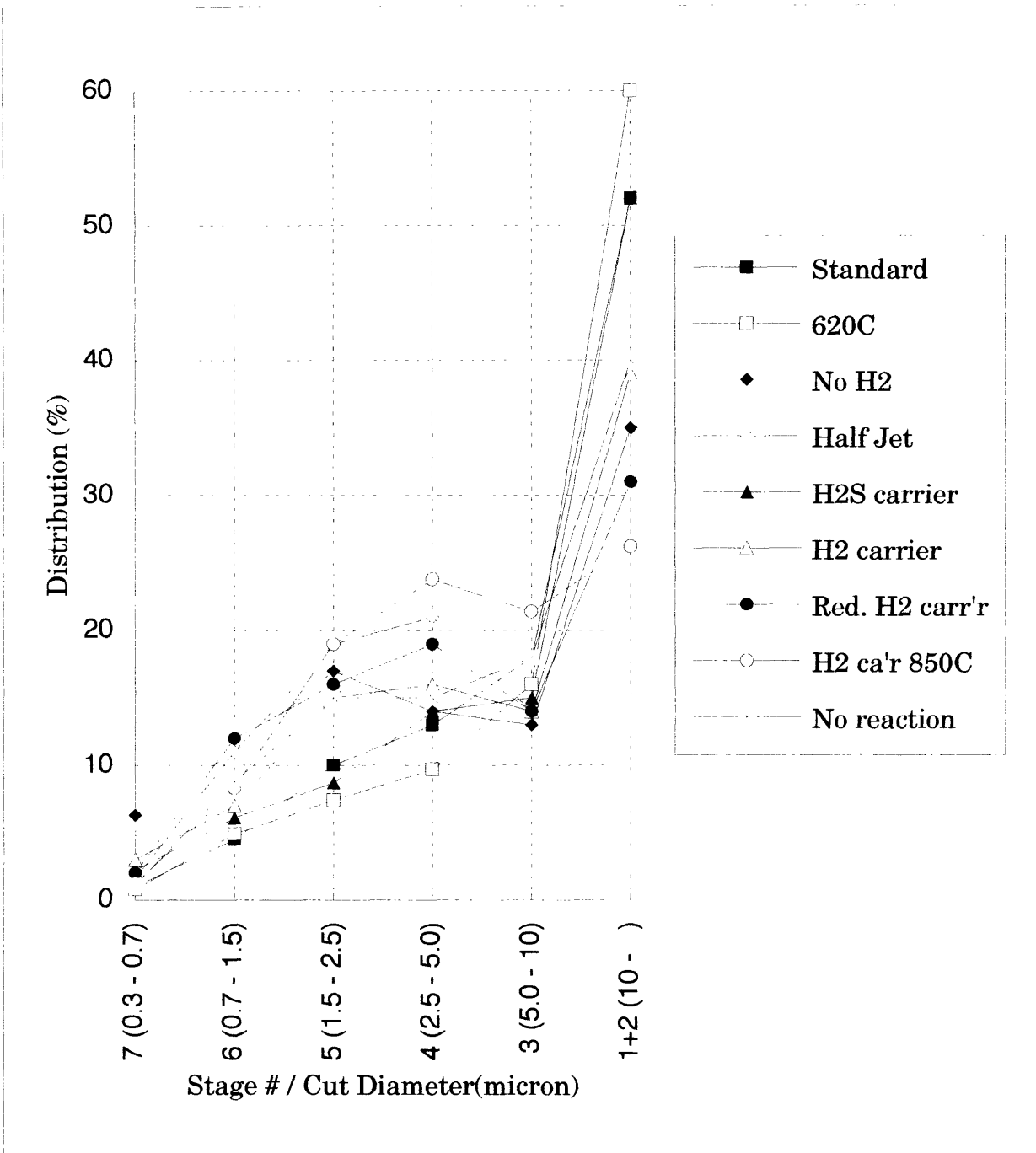


Figure 3.11 Particle Size Distribution of Reacted ZnO-2 Sorbent

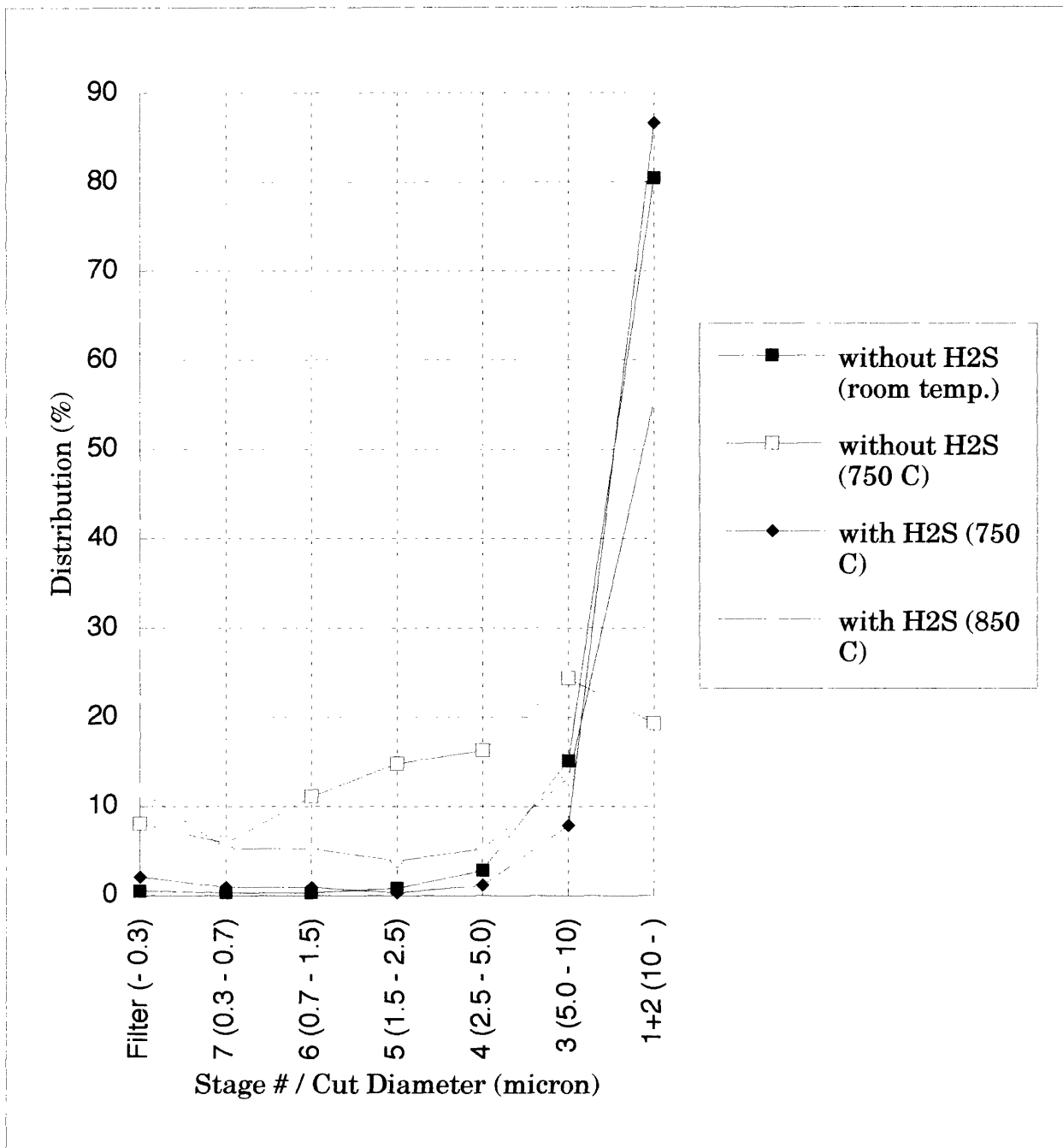


Figure 3.12 Particle Size Distribution of Reacted Metallic Zn

completely. This suggests that vaporization of metallic zinc is suppressed by H_2S because of the formation of ZnS layer on the particle surface and/or immediate deposition of gas phase formed ZnS onto the original particle surface. The size distribution after sulfidation at 850°C (case d)) was in between case b) and c) and the amount of the fine powder under stage 7 (smaller than $0.3\ \mu\text{m}$) was the most among all the cases. However, judging from the color, almost all of the powder under stage 4 (smaller than $2.5\ \mu\text{m}$) was ZnS , not metallic Zn . This shows that vaporization at 850°C was so rapid that some of the vaporized Zn exists far enough from the original surface to form independent fine powder of ZnS by gaseous sulfidation with H_2S .

Judging from the fact that the vaporization of metallic Zn was effectively suppressed by H_2S even with metallic zinc powder as the starting material, which simulated an extreme case with very rapid reduction rate of sorbent, H_2S seem to suppress mainly the vaporization by immediate formation of ZnS , not the reduction reaction itself.

3.4.3 Effect of Gas Composition and Carrier Gas

Figure 3.13 shows a comparison of sulfidation conversion of ZnO-2 sorbent with various different gas conditions shown below, i.e. selection of carrier gas, bulk flow velocity, and jet flow velocity.

- a) 620°C , Carrier : CO_2
- b) 750°C , Carrier : CO_2
- c) 750°C , Carrier : CO_2 , No H_2 in reactant gas
- d) 750°C , Carrier : CO_2 , Half jet flow rate
- e) 750°C , Carrier : 6% H_2S
- f) 750°C , Carrier : 6% H_2S , Doubled bulk flow rate
- g) 620°C , Carrier : H_2
- h) 750°C , Carrier : H_2
- i) 850°C , Carrier : H_2

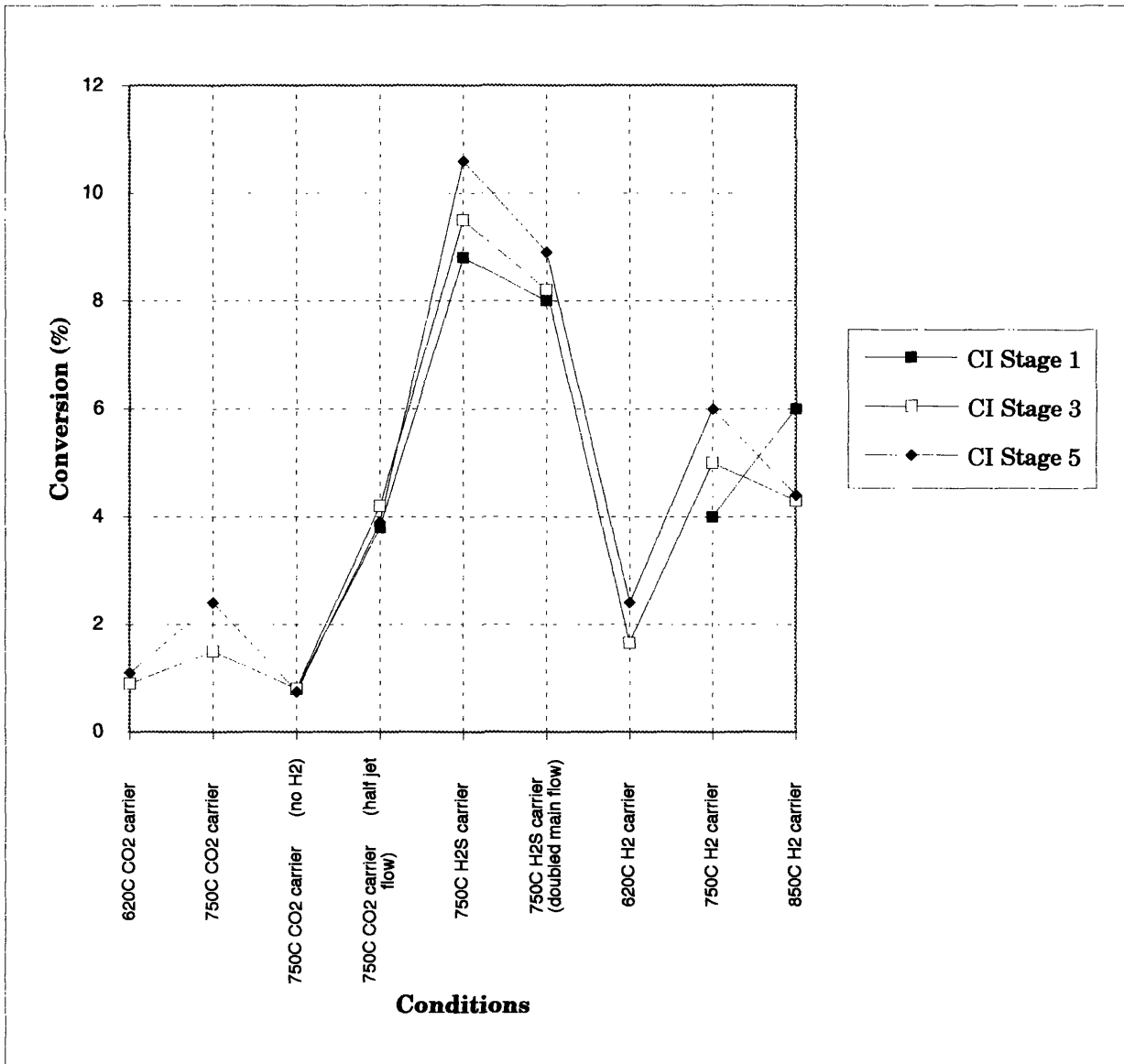


Figure 3.13 Sulfidation Conversions of ZnO-2 Sorbent

Common experimental conditions;

H₂S concentration : 1.0%

H₂ concentration : 20% (except case c)

CO₂ concentration : 18%

Jet flow velocity : 97 cm/s (except case d)

Bulk flow velocity : 5 cm/s (except case f)

Reaction zone length : 10 cm

The results are summarized as follows;

- (1) When 6% H₂S/N₂ was used as the carrier gas, conversions were 4.5-6.3 times higher than the cases with CO₂ as the carrier even though in both cases, the bulk concentration of H₂S was 1% and there was no other difference in gas composition or velocity.**
- (2) When H₂ was used as the carrier gas, conversions were about twice or more as high as the cases with CO₂ as the carrier.**
- (3) When there was no H₂ in the bulk gas, conversions were roughly halved.**
- (4) By halving the jet flow (decrease in the total gas flow was only 8%), conversions were almost doubled.**
- (5) By doubling the bulk flow rate with 6% H₂S as the sorbent carrier, conversions decreased only slightly.**

As a previous study (Lew et.al. 1992) showed that the sulfidation reaction rate was first order of H₂S concentration, the result (1) shows that there was a significant gradient of H₂S concentration around the sorbent particles in the reaction zone, that is, mixing effect was not negligible.

The results (2) and (3) suggest that H₂ had an enhancing effect on sulfidation reaction. The effect of H₂ may be enhancement of surface reaction by previous reduction of ZnO or promotion of gaseous mixing with its high diffusivity. From the fact that the difference of conversion between H₂ carrier

and CO₂ carrier was almost the same at 620°C and 750°C, promotion of mixing seems to be the main cause of the enhancement because the effect of reduction reaction should be more significant at higher temperature with its much higher activation energy than sulfidation.

The results (4) and (5) suggest that the jet flow rate has more dominant effect on reaction than the bulk flow, that is, the overall retention time of a particle in the reaction zone depends mainly on the jet flow, not on the bulk flow. This means that the length required for the particle velocity, which is initially the same as the jet flow, to reach the bulk flow velocity is longer than the length of the reaction zone.

Based on the above results, a model of mixing of jet and bulk flows was formulated and examined in Chapter 4.

3.4.4 Effect of the Length of Reaction Zone

Figure 3.14 shows the relationship between sulfidation conversion of ZnO-2 sorbent and the length of the reaction zone at 750°C and with 1 vol% H₂S. Figure 3.14 also shows the effect of sorbent particle size. Sorbent carrier was CO₂ in those experiments. As mentioned before, however, the experiments with 30 cm reaction zone had a problem of nonuniform temperature. The conversion was close to zero with 5 cm reaction zone length. This was also the same at higher (~910°C) temperature and with higher (~4 vol%) H₂S concentration. It is clear that an “inlet region” in which mixing of jet and bulk flows is insufficient exists and the length of the “inlet region” is longer than 5 cm but shorter than 10 cm.

3.4.5 Effect of Temperature

Figure 3.15 and 3.16 are the Arrhenius plots of sulfidation of ZnO-2

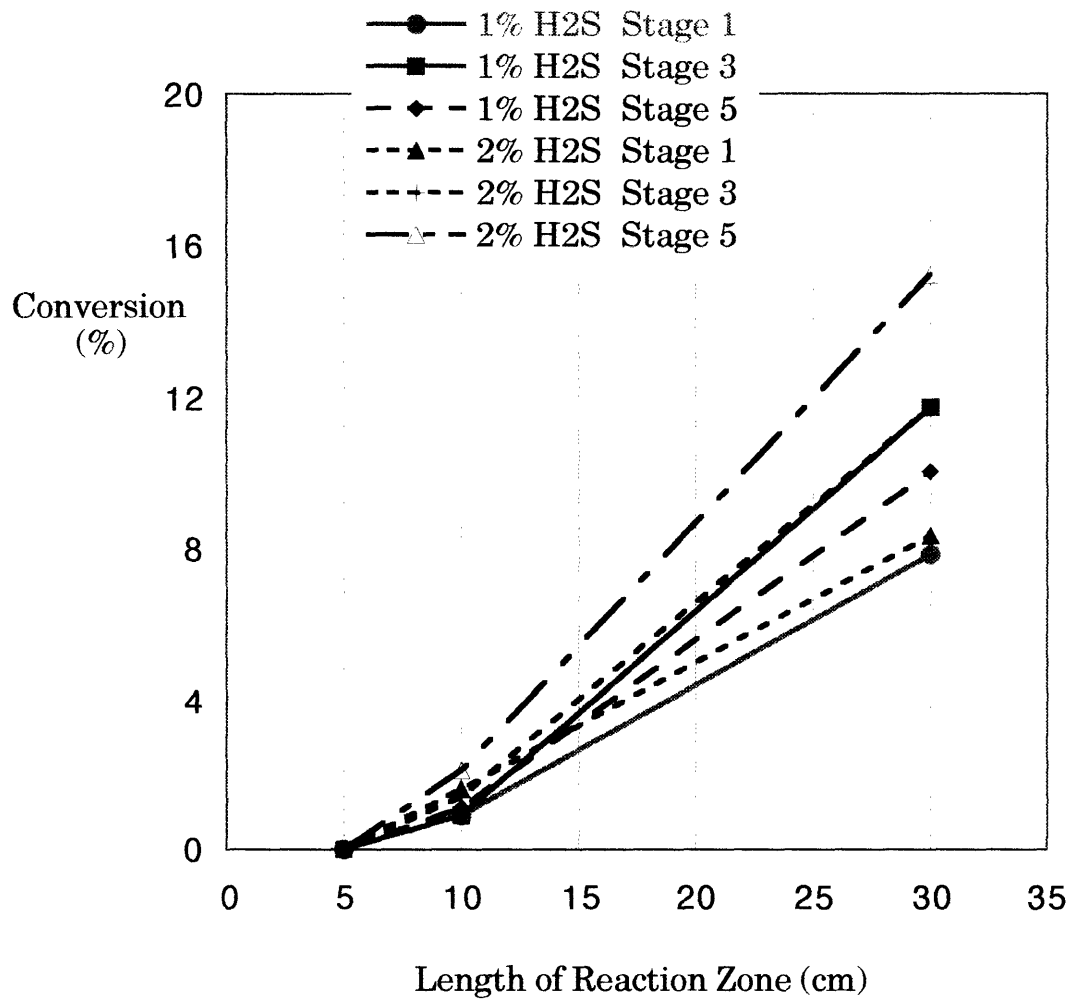


Figure 3.14 Sulfidation Conversions with Different Reaction Zone Length

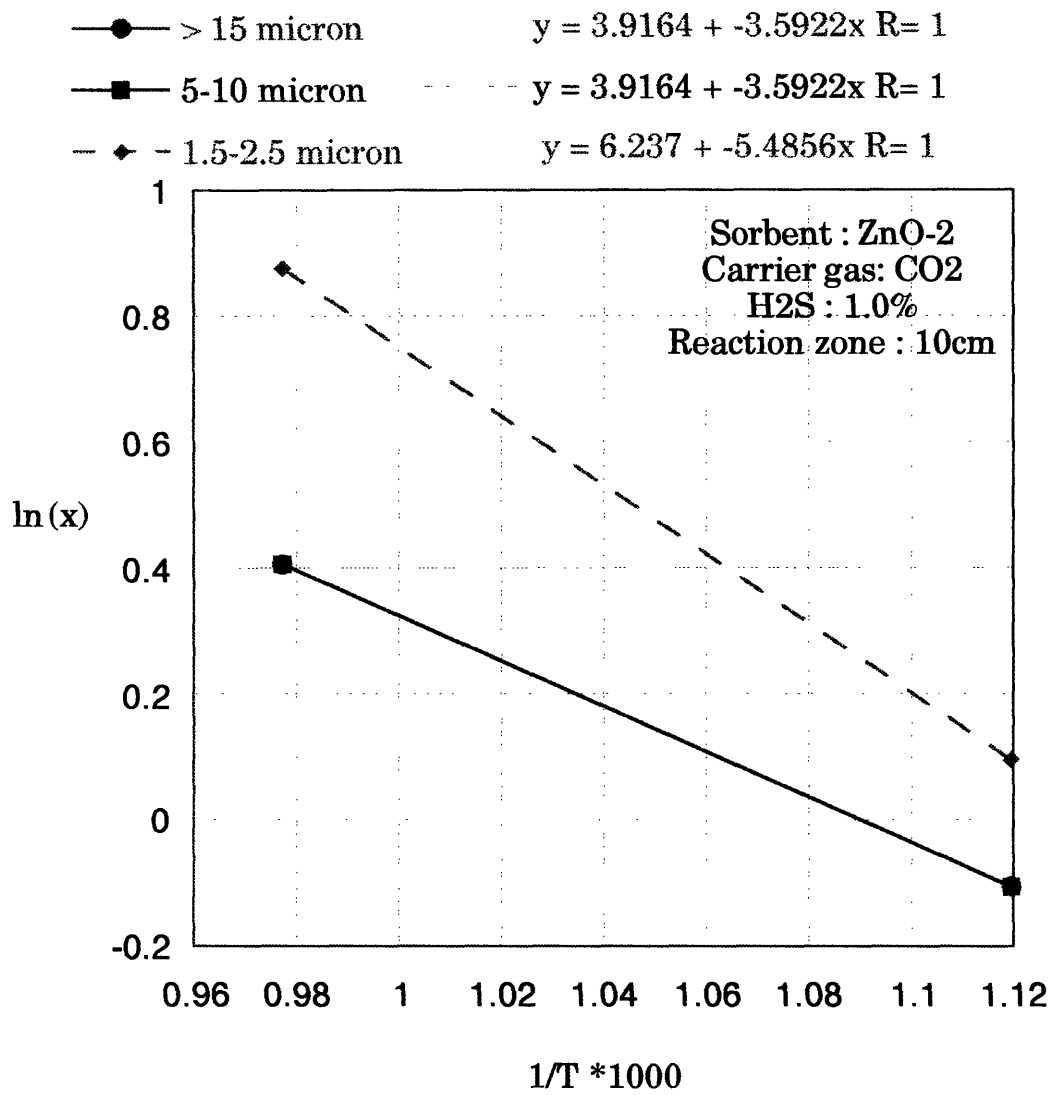


Figure 3.15 Arrhenius Plot of ZnO-2 Sulfidation (Sorbent Carrier : CO2)

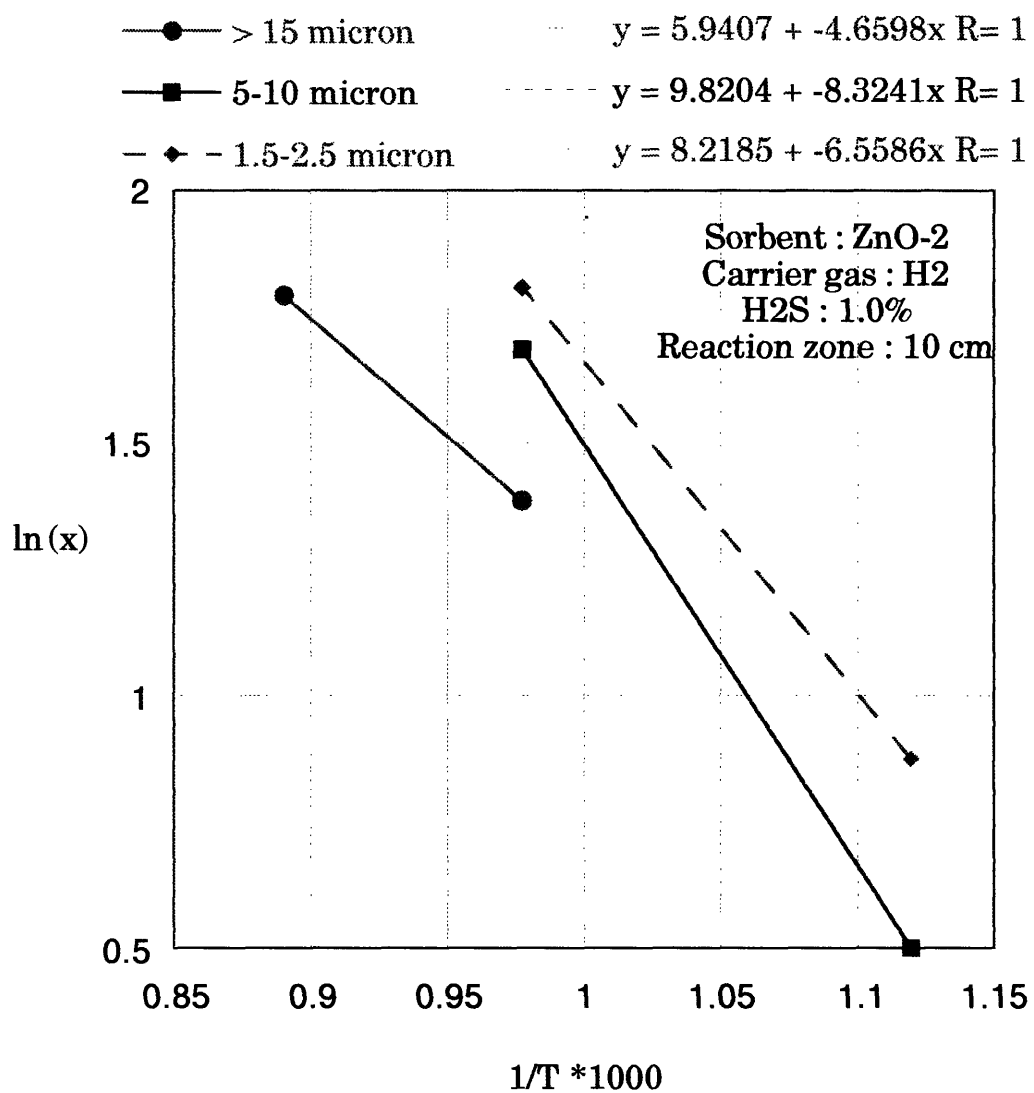


Figure 3.16 Arrhenius Plot of ZnO-2 Sulfidation
(Sorbent Carrier : H2)

sorbent for the sorbent particle sizes of 1.5-2.5, 5-10, and >15 μm . The sorbent carrier was CO_2 or H_2 . Assuming that the surface reaction is the rate limiting step and that the other factors such as gas composition gradient and particle velocity are not influenced by temperature, the difference of conversion directly indicates the difference of reaction rate coefficient.

From the Arrhenius plots for each particle size and sorbent carrier gas, activation energy was calculated as shown in Table 3.2. The activation energy of the reaction,



was reported as 10.3 kcal/mol for the temperature range of 400~700°C (Lew et.al. 1992) and 7.2 kcal/mol for 300~750°C (Westmoreland et al. 1977).

3.4.6 Particle Size Dependence

Figure 3.13 and 3.14 also show the difference in sulfidation conversion among three different sizes of the ZnO-2 sorbent particle, that is, 1.5~2.5, 5~10, and >15 μm . Based on these particle size dependence of sulfidation conversion, a kinetic model of single sorbent particle sulfidation is examined in the next section. In these experiments with 10 cm reaction zone, however, particle size distribution of sulfidation conversion was much less significant than the experiments with 30 cm reaction zone. Though reaction zone as long as 30 cm has a problem in uniformity of temperature, longer reaction zone than 10 cm may be desirable for the study of size dependence. This is because with short reaction zone, there may be a significant variation of the particle velocity which may make the size dependence unclear.

3.5 Comparison of Different Sorbents

Table 3.2 Actination Energy of ZnO-2 Sulfidation

Carrier Gas	Particle Size (μ)	Slope of Arrhenius Plot	Ea (kcal/mol)
CO ₂	1.5 ~ 2.5	- 5490	10.9
	5 ~ 10	- 3590	7.1
	> 15	- 3590	7.1
H ₂	1.5 ~ 2.5	- 6560	13.0
	5 ~ 10	- 8320	16.5
	> 15	- 4660	9.3

3.5.1 Test Results

Table 3.3 shows the sulfidation conversions of ZnO-2, ZnO(Johnson Matthey), and ZnTiO₃(Pfaltz & Bauer) sorbents at the same reaction condition.

The difference between two types of ZnO mainly depends on the surface area. Neglecting the factor of diffusion in sorbent particles, surface reaction rate per surface area for 5 - 10 μm particle size is $1.60\text{E-}8$ mol/cm²s for ZnO-2 and $1.84\text{E-}8$ mol/cm²s for ZnO(Johnson Matthey).

3.5.2 Comparison of ZnO and Zinc Titanate Sorbents

The difference between ZnO-2 and zinc titanate depends on both the surface area and the frequency factor with existence of titanate. Neglecting the factor of diffusion in sorbent particles as above, surface reaction rate per surface area for 5 - 10 μm particle size is $1.60\text{E-}8$ mol/cm²s and $0.70\text{E-}8$ mol/cm²s for ZnO-2 and ZnTiO₃(Pfaltz & Bauer), respectively. Reduction of ZnO seems to have little enhancement effect on overall sulfidation reaction at 750°C. However, because the reduction of ZnO is not to be a problem in the case of sorbent injection process, ZnO seems to be a better sorbent for this process than zinc titanate for its faster sulfidation rate and higher sulfur loading capacity, that is, higher desulfurization performance.

Table 3.3 Sulfidation Conversions of ZnO and Zinc Titanate Sorbents

Sorbent	Particle diameter (μm)	Conversion (%)
ZnO-2	> 15	4.0
(M.I.T.)	5~10	5.2
ZnO	> 15	0.12
(Johnson Matthey)	5~10	0.6
ZnTiO ₃	> 15	0.9
(Pfaltz & Bauer)	5~10	1.6

(Experimental Conditions)

Temperature	750°C
Gas Compositions	H ₂ S 1.0% - H ₂ 20% - CO ₂ 18% - N ₂ balance
Sorbent Carrier	H ₂ (pure)
Jet Flow	97 cm/sec
Bulk Flow	5 cm/sec
Reaction Zone Length	10 cm

3.6 Conclusions

- 1) At 750°C or lower temperature, H₂S was found to almost completely inhibit the size decrease of sorbent particles caused by vaporization of metallic Zn formed by reduction of ZnO with H₂. This effect seems to be mainly suppression of zinc vaporization, not the reduction reaction.

- 2) At 850°C, fine particles less than 0.3 μm in diameter were formed even in the presence of H₂S. These fine particles were found to be ZnS formed by the reaction of vaporized zinc and H₂S and would be possibly captured by micro filtration. Therefore, at this temperature, vaporization of zinc and formation of fine particles aids the conversion of the sorbent. At the same time, capture of the ZnS fines by the ceramic filter avoids downstream problems.

- 3) The effect of reduction reaction enhancing overall sulfidation conversion was not observed in experiments at temperatures up to 750°C. This becomes appreciable above 800°C (see (2) above).

- 4) Gas mixing in the drop-tube reactor was revealed to be not rapid enough to enable the assumption of complete mixing; therefore, for a quantitative study of the reaction kinetics, a mixing model of the reactor is required. This is examined in the following chapter,

CHAPTER 4

MODELING OF SULFIDATION

4.1 Introduction

As shown in the previous chapter, the drop-tube reactor cannot be assumed as a perfectly mixed reactor, that is, large gradients of gas composition and particle velocity exist in the reaction zone. Therefore, in order to examine the reaction kinetics of the sorbent quantitatively, a mixing model of the drop-tube reactor is required. The mixing model was based on the results of sulfidation experiments of ZnO-2 sorbent, diffusion coefficients of the components of the reactant gas, and assumptions that the sulfidation reaction is first order in H₂S and that the surface reaction is the rate limiting step.

After the mixing model was fixed, reaction model of single sorbent particle was examined. The model was based on the grain model which had been reported to fit well the experimental results of ZnO sulfidation reaction (Lew et al. 1992). Two approaches were tried, that is, to obtain an appropriate diffusion coefficient of reactants in solid phase assuming the grain size was equal to the particle size which was classified by the cascade impactor, and to obtain an appropriate grain size by fixing diffusion coefficients at reported values. In both cases, particle size dependence of sulfidation conversion should be explained by the model.

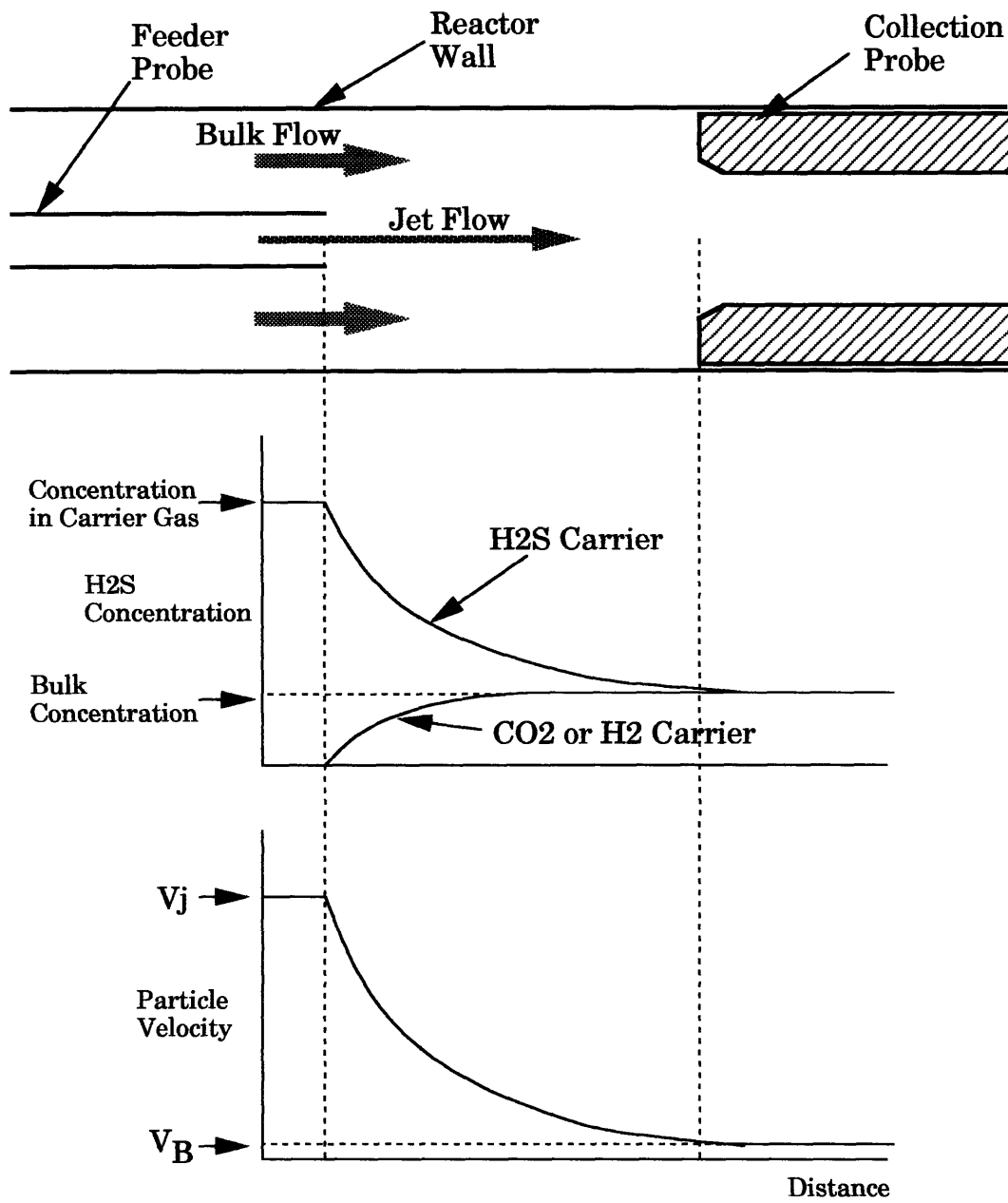
4.2 Modeling of Mixing in the Drop-Tube Furnace

4.2.1 The Concentration Distribution of H₂S in the Reaction Zone

Figure 4.1 shows a concept of the mixing model in the drop-tube reactor. The reaction zone begins at the edge of the feeding probe where the jet flow comes into the bulk flow. As a simplified model, the jet flow was considered as a cylindrical flow which maintains its diameter and flow velocity while the bulk flow, the velocity of which was about 5 % of the jet flow, was considered stagnant. In this model, the extent of mixing depends on diffusion of gas components from bulk into the cylinder of the jet flow. Assuming that there is no radial gradient in the jet flow, axial gradient of concentration of H₂S in the jet flow was calculated for each carrier gas using binary diffusion coefficients of H₂S and the carrier gas. Table 4.1 shows the binary gas coefficients used in the calculation.

Table 4.1 Binary Diffusion Coefficients of Gas Components

Pair of Components	De = A * T ^B (cm ² /s)		De at 20°C (cm ² /s)	De at 750°C (cm ² /s)
	A	B		
H ₂ S - H ₂	3.474E-5	1.728	0.625	5.473
H ₂ S - CO ₂	3.839E-6	1.817	0.1131	1.110
H ₂ S - N ₂	8.437E-6	1.738	0.1607	1.427
H ₂ - CO ₂	3.758E-5	1.707	0.603	5.129
H ₂ - N ₂	5.357E-5	1.675	0.721	5.877
CO ₂ - N ₂	8.960E-6	1.715	0.1502	1.292



A model of jet flow

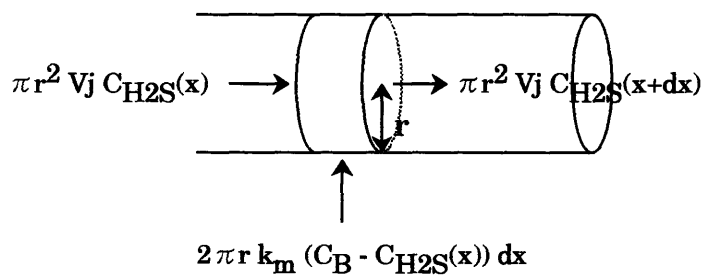


Figure 4.1 Mixing Model of the Drop-tube Reactor

The concentration of H₂S in the jet flow is expressed as a function of the distance from the inlet as;

$$C_{H_2S} = C_B \left(1 - \exp \left(- \frac{2 De}{v r^2} x \right) \right) \quad \text{---- (4.1)}$$

where

- C_{H₂S} : H₂S concentration in the jet flow (%)
- C_B : H₂S concentration in the bulk flow (%) --- constant
- De : Binary diffusion coefficient of H₂S and carrier gas (cm²/s)
- v : Jet flow velocity (cm/s)
- r : Jet flow radius (cm)
- x : Distance from jet inlet (cm)

From the equation, distance at which C_{H₂S} becomes 90% of C_B can be calculated for various conditions. The results are shown below;

	x (cm) at	
	<u>C_{H₂S} / C_B = 0.5</u>	<u>C_{H₂S} / C_B = 0.9</u>
a) 620°C, Carrier : CO ₂	1.53	5.08
b) 750°C, Carrier : CO ₂	1.21	4.02
c) 750°C, Carrier : CO ₂ (half jet flow rate)	0.61	2.01
d) 620°C, Carrier : H ₂	0.31	1.02
e) 750°C, Carrier : H ₂	0.25	0.82

At both 620 and 750°C, x with CO₂ as the carrier gas is about 5 times longer than x at the same C_{H₂S} / C_B ratio with H₂ as the carrier gas. In the cases with CO₂ as the carrier gas, it is obvious that x at C_{H₂S} / C_B = 0.9 is not negligible compared to the length of reaction zone, 10 cm.

If the velocity of sorbent particles is constant throughout the reaction zone and the reaction rate of sulfidation is first order in H₂S, sulfidation

conversion of a sorbent particle at the outlet is proportional to the integral of C_{H_2S} in the reaction zone. From Eq. 4.1,

$$\int_0^L C_{H_2S} dx = \int_0^L C_B \left(1 - \exp\left(-\frac{2 De}{v r^2} x\right) \right) dx$$

$$= C_B \left(L + \frac{v r^2}{2 De} \left(1 - \exp\left(-\frac{2 De}{v r^2} L\right) \right) \right) \quad \text{---- (4.2)}$$

The values of the integral for above experimental conditions are;

$$\int_0^L C_{H_2S} dx \quad (C_B * (cm))$$

a) 620°C, Carrier : CO ₂	4.02 C _B
b) 750°C, Carrier : CO ₂	4.69 C _B
c) 750°C, Carrier : CO ₂ (half jet flow rate)	6.73 C _B
d) 620°C, Carrier : H ₂	8.23 C _B
e) 750°C, Carrier : H ₂	8.58 C _B

The above values of the integrated concentration of H₂S roughly coincide with the test result that the conversions with H₂ as the sorbent carrier were about twice as high as the cases with CO₂ as the sorbent carrier at both 620 and 750°C. However, the integrated concentration of H₂S does not explain why the conversions were higher with half the jet flow rate (case c). This suggests that the jet flow velocity affects not only the diffusion of H₂S but also the retention time of sorbent particles in the reaction zone. The latter factor may have rather stronger effect on sulfidation conversion.

4.2.2 The Velocity of Sorbent Particles in the Reaction Zone

As mentioned in the previous section, the jet flow rate seems to have strong effect on the retention time of sorbent particles in the reaction zone. In other words, the length required for the particle velocity, which is initially the same as the jet flow, to reach the bulk flow velocity is long enough, in comparison to the length of the reaction zone, to affect sulfidation conversion of sorbent particles.

It can be assumed that, as the concentration distribution, the velocity of a particle emitted in the jet flow decreases exponentially to reach the bulk velocity, that is;

$$v_P = v_B + (v_j - v_B) \exp(-kx) \quad \text{---- (4.3)}$$

where v_P : Particle velocity (cm/s)
 v_j : Initial particle velocity = jet flow velocity (cm/s)
 v_B : Bulk flow velocity (cm/s)
 k : constant
 x : Distance from jet inlet (cm)

The retention time of a particle in the reaction zone can be obtained by integrating dx/v_P throughout the zone, that is;

$$t = \int_0^L dx/v_P = \int_0^L dx/(v_B + (v_j - v_B) \exp(-kx))$$

$$= \frac{L}{v_B} + \frac{1}{v_B k} \ln\left(\frac{v_B + (v_j - v_B) \exp(-kL)}{v_j}\right) \quad \text{---- (4.4)}$$

t : retention time (sec)

If “k” is assumed to be constant when v_j , gas composition, and temperature are the same, “t” can be calculated as a function of “k” for two experimental

conditions of ZnO-2 sulfidation at 750°C in which v_B was the test parameter.

- a) Jet flow : 97 cm/s, Bulk flow : 5 cm/s
 - b) Jet flow : 97 cm/s, Bulk flow : 10 cm/s
- Reaction zone length : 10 cm

The results are shown in Figure 4.2.

From the drop-tube experiments, sulfidation conversions in case b) was 84 ~ 90 % of case a) depending on particle size. Assuming that this difference in conversion corresponds only to the retention time of the sorbent particles, the value of k should be around 0.2 from Figure 4.2. Applying $k=0.2$ into Eq. 4.3,

$$v_P = v_B + (v_j - v_B) \exp(-0.2x) \quad \text{---- (4.5)}$$

$(v_P - v_B)$ becomes 50% of $(v_j - v_B)$ at $x=2.3$ and 10% of $(v_j - v_B)$ at $x=11$. In other words, the difference of particle and bulk flow velocity $(v_P - v_B)$ is still 14% of $(v_j - v_B)$ at the outlet of the reaction zone.

4.2.3 Summary of The Mixing Model in the Drop-Tube Furnace

The distribution of H_2S concentration and particle velocity in the reaction zone in the drop-tube reactor was obtained from experimental results of sulfidation of ZnO-2 sorbent. These models are somewhat rough, though, particularly the particle velocity model which should include particle size dependence. However, for the purpose of compensating the deviation from the complete mixing model for more accurate modeling of sulfidation reaction of single sorbent particle, these models are considered useful.

Figure 4.3 shows the distribution of H_2S concentration and particle velocity in the reaction zone at a “standard” experimental condition, that is, at 750°C, jet flow is 97 cm/s, bulk flow is 5 cm/s, reaction zone length is 10 cm,

- a) Jet flow : 97 cm/s, Bulk flow : 5 cm/s
- b) Jet flow : 97 cm/s, Bulk flow : 10 cm/s

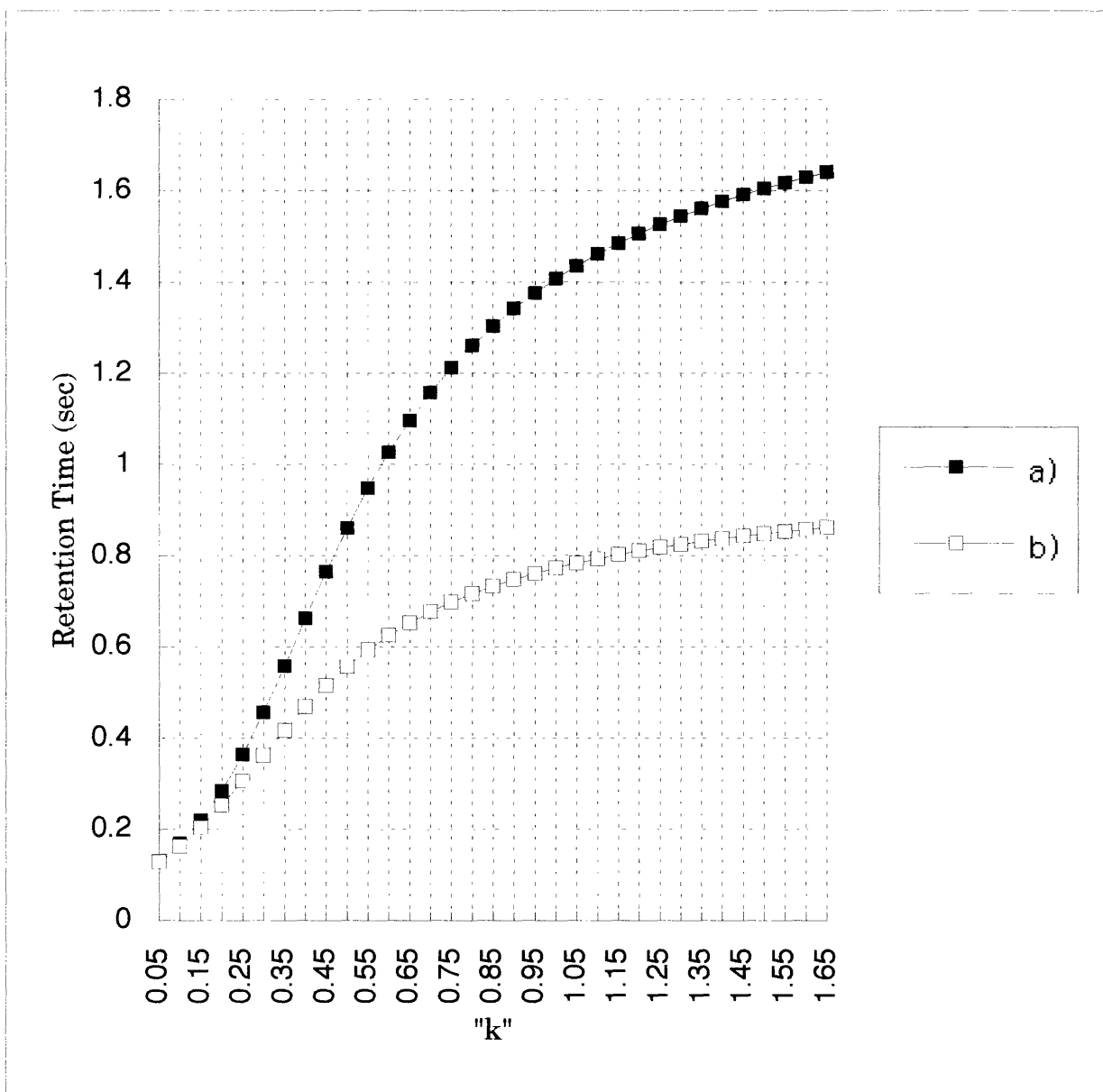


Figure 4.2 " k " vs. Retention Time

Temp.: 750degC, Jet flow : 97 cm/s, Bulk flow : 5 cm/s
 Reaction zone length : 10 cm

CH2S = $CB(1-\exp(-2De x / v / r^2))$

a) H2 carrier : $De = 5.473$

b) CO2 carrier : $De = 1.110$

$V_p = V_B + (V_j - V_B)\exp(-0.2x) = 5 + 92\exp(-0.2x)$

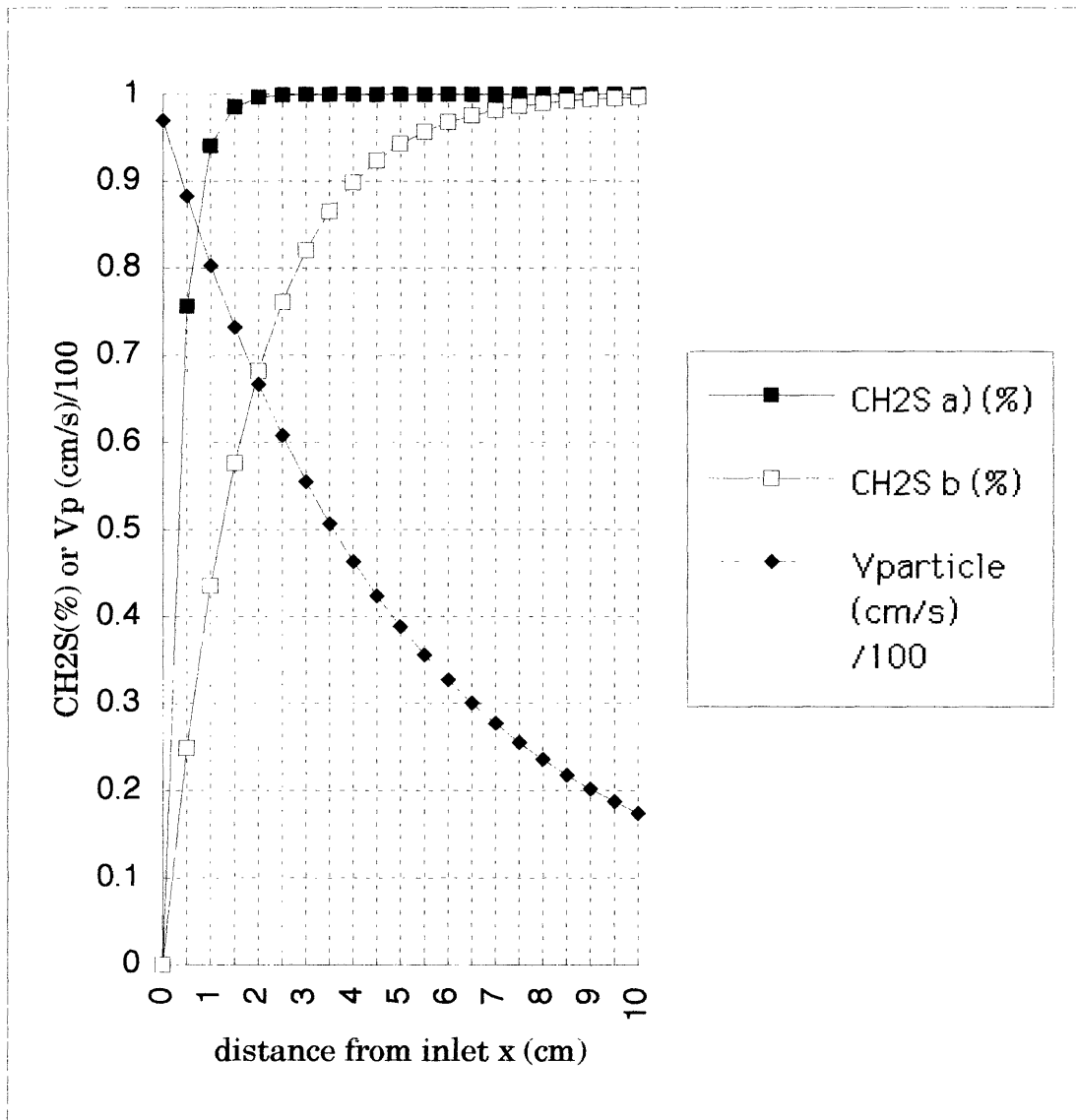


Figure 4.3 Distribution of H2S concentration and particle velocity in the reaction zone

and the sorbent carrier is CO₂ or H₂. The results show that the retention time of a sorbent particle in the reaction zone is about 0.3 sec, significantly shorter than that of the bulk flow, i.e. 2 sec, but three times longer than that calculated from the jet flow velocity, i.e. 0.1 sec.

4.3 Modeling of the Gas - Solid Sulfidation Reaction

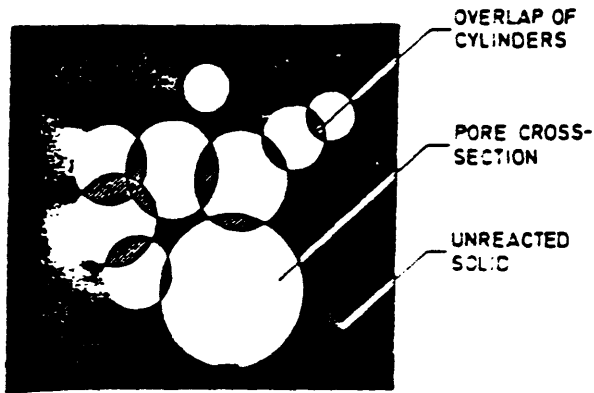
4.3.1 Introduction

There are several mathematical models which can express the kinetics of gas-solid reaction. Most of them can be classified in two large groups, i.e. grain models or pore models. Grain models represent porous solid material as an assemblage of small grains while pore models represent the solid as a collection of small pores. Figure 4.4 shows examples of grain and pore models(Lew et al. 1990). The most fundamental difference between grain models and pore models is the expression of reactant surface area and pore surface area. While reactant surface area and pore surface area decrease monotonously with conversion in grain models, in pore models there exists a maxima in reaction surface area because pore diameter increases with reaction. It was reported that a simple grain model expressed the sulfidation of porous ZnO very well(Lew et al. 1990); therefore, a grain model was examined and applied to express the experimental results in this section.

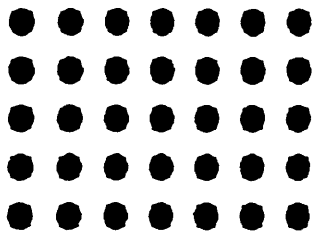
One concern about applying the grain model is that in most experiments, the conversions were only several %, possibly too low to look at the effect of diffusion. For comparison, a surface reaction limitation model in which no diffusion resistance is assumed to exist was also examined.

4.3.2 Surface Reaction Limitation Model

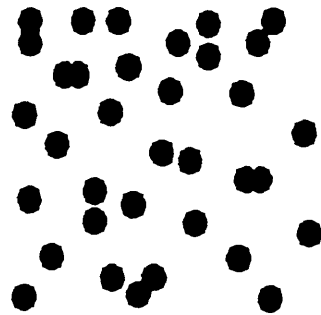
This is an extreme model in which it is assumed that there is no



a) Random Pore Model with a distributed pore size
(from Bhatia and Perlmutter, 1980)



b) Grain Model



c) Random Grain Model
(uniform spherical grains)

● unreacted solid

Figure 4.4 Schematic Representations of the Reacting Porous Solid by
a) Random Pore, b) Simple Grain, and c) random Grain Models

limitation by diffusion (gas phase, pore, product layer). Particles are so porous that no concentration gradient exists in the particle and reaction occurs on all the surface at the initial reaction rate. As the initial reaction rate, a reported value for ZnO sulfidation (Lew et al. 1990) was used. A sorbent particle was assumed to be a sphere with uniform diameter and porosity. In this model, particle size dependence is expressed as the difference in the surface area because the smaller the particle becomes, the more dominant the outer surface of the particle becomes and, then, the larger the total surface area is.

Model Expression (using the bulk surface area --- no size dependence):

(reaction rate of a single particle)

$$\begin{aligned}
 &= (\text{initial reaction rate}) * (\text{surface area of the particle}) \\
 &= (\text{mole number of Zn in the particle}) * \frac{dx}{dt}
 \end{aligned}$$

$$\begin{aligned}
 \rightarrow R * \left(\frac{4}{3} \pi r^3 \phi a \right) (1-x) &= k C_{H_2S} * \left(\frac{4}{3} \pi r^3 \phi a \right) (1-x) \\
 &= \left(\frac{4}{3} \pi r^3 \phi \frac{1}{M} \right) \frac{dx}{dt} \quad \text{---- (4.6)}
 \end{aligned}$$

where, $R = k C_{H_2S}$: initial reaction rate (mmol/cm² s)
 r : particle radius (cm)
 ϕ : particle density = 1.1 g/cm³
 a : bulk surface area = 2.0 m²/g
 x : sulfidation conversion (-)
 M : molecular weight of ZnO
 t : reaction time (sec)

Eq. 4.6 can be simplified as,

$$k C_{H_2S} a M dt = \frac{dx}{1-x} \quad \text{---- (4.7)}$$

By integration,

$$x = 1 - \exp(-k C_{H_2S} a M t) \quad \text{---- (4.8)}$$

The result of the calculation is shown in Figures 4.5 and 4.6 for 0.4% H₂S and 1% H₂S, respectively.

The above model is based on the bulk surface area of the sorbent. In the case of fine particles, the outer surface of the particle becomes dominant and the total surface area increases. If a particle is assumed to be a sphere,

Outer surface area : $S_o = 4 \pi r^2$ (cm²)

Inner surface area : $S_i = 4/3 \pi r^3 \phi a$ (cm²)

Total surface area per unit weight :

$$\begin{aligned} At &= (S_o + S_i) / (4/3 \pi r^3 \phi) \quad (\text{cm}^2/\text{g}) \\ &= a + 3 / (r \phi) \end{aligned} \quad \text{---- (4.9)}$$

where, r : particle radius (cm)

ϕ : particle density

a : bulk surface area

At was calculated for ZnO-2 ($a = 2.0 \text{ m}^2/\text{g}$, $\phi = 1.1 \text{ g}/\text{cm}^3$) and Johnson Matthey ZnO ($a = 0.2 \text{ m}^2/\text{g}$, $\phi = 2.0 \text{ g}/\text{cm}^3$) as follows;

Stage of Cascade Impactor	1	3	5	Filter
Average Radius (cm)	$3 \cdot 10^{-3}$	$8 \cdot 10^{-4}$	$2 \cdot 10^{-4}$	$3 \cdot 10^{-5}$
At (cm ² /g) [ZnO-2]	2.18	2.68	4.75	20.3
[J. M. ZnO]	0.30	0.58	1.70	10.2

From the assumptions, sulfidation conversion of each particle size is proportional to the surface area. Calculated values of A_t show that in the case of ZnO-2 sorbent, the conversion of the particles captured on Stage 5 of the cascade impactor should be about twice of that of Stage 1 and that ZnO-2 should have roughly one order of magnitude higher conversions than Johnson Matthey ZnO. These roughly coincided with the experimental results.

4.3.3 Simple Grain Model

In this model, each sorbent particle is assumed to be an agglomerate of non-porous fine grains. As each grain is assumed to be non porous, grain size can be derived from the value of surface area and density of the sorbent. In the case of porous ZnO sorbent, the grain radius calculated this way is $0.22\mu\text{m}$. Each grain reacts according to the shrinking core model with an assumed value of the product layer diffusion coefficient D_e .

As the grain radius of $0.22\mu\text{m}$ is much smaller than the sorbent particles, particle size dependence observed in the drop-tube experiments among the particles with diameter of $1.5\sim 2.5$, $5\sim 10$, and $>15\mu\text{m}$ cannot be expressed no matter what value of D_e is selected. Therefore, another grain model in which each particle itself is assumed to be a non-porous grain was also examined.

In both grain models, each grain was assumed to be a uniform sphere and the same value of the initial reaction rate as the surface reaction limitation model was used. No sintering or breaking of grains was considered.

Model expression;

$$\frac{b k}{\phi r_0} C_{A0} t = 1 - (1-x)^{1/Fg} + \frac{k r_0}{2 Fg D_e} \left(\frac{Z - (Z+(1-Z)(1-x))^{2/3}}{Z - 1} - (1-x)^{2/3} \right) \quad -- (4.9)$$

where, x : conversion
 Z : volume of formed product per unit volume of reactant
 r_0 : initial grain size
 F_g : grain size factor (3 for sphere)
 D_e : product layer diffusion coefficient
 k : rate constant
 C_{A0} : bulk concentration of gaseous reactant

The result of the calculation is shown and compared with the surface reaction limitation model in Figure 4.5 and 4.6 for 0.4% H₂S and 1% H₂S, respectively.

4.4 Comparison of Models and Experimental Results

4.4.1 Comparison of Grain and Reaction Limiting Models

As Figure 4.5 and 4.6 show, calculated result of the grain model with 0.22 μm was very close to the result of the reaction limiting model. Those two models are considered to be extreme cases with very low diffusion resistance. For larger grain sizes, there was a significant difference in conversion. At the same reaction time, the conversion of 0.5 μm radius grain was about one order of magnitude larger than 5 μm radius grain. In grain models, two values of D_e were used. One was a value reported for a porous ZnO sorbent, and another was this value times 10^6 to look at the difference in size dependence of conversion. The effect of the increased value of D_e was not so much and strong size dependence of conversion still remained even with the large value of D_e .

4.4.2 Comparison of Models and Experimental Results

Figure 4.7 shows a comparison of the reaction models and experimental results at a very low conversion - short term scale. As mentioned in the previous chapter, there were gas composition and particle size gradients

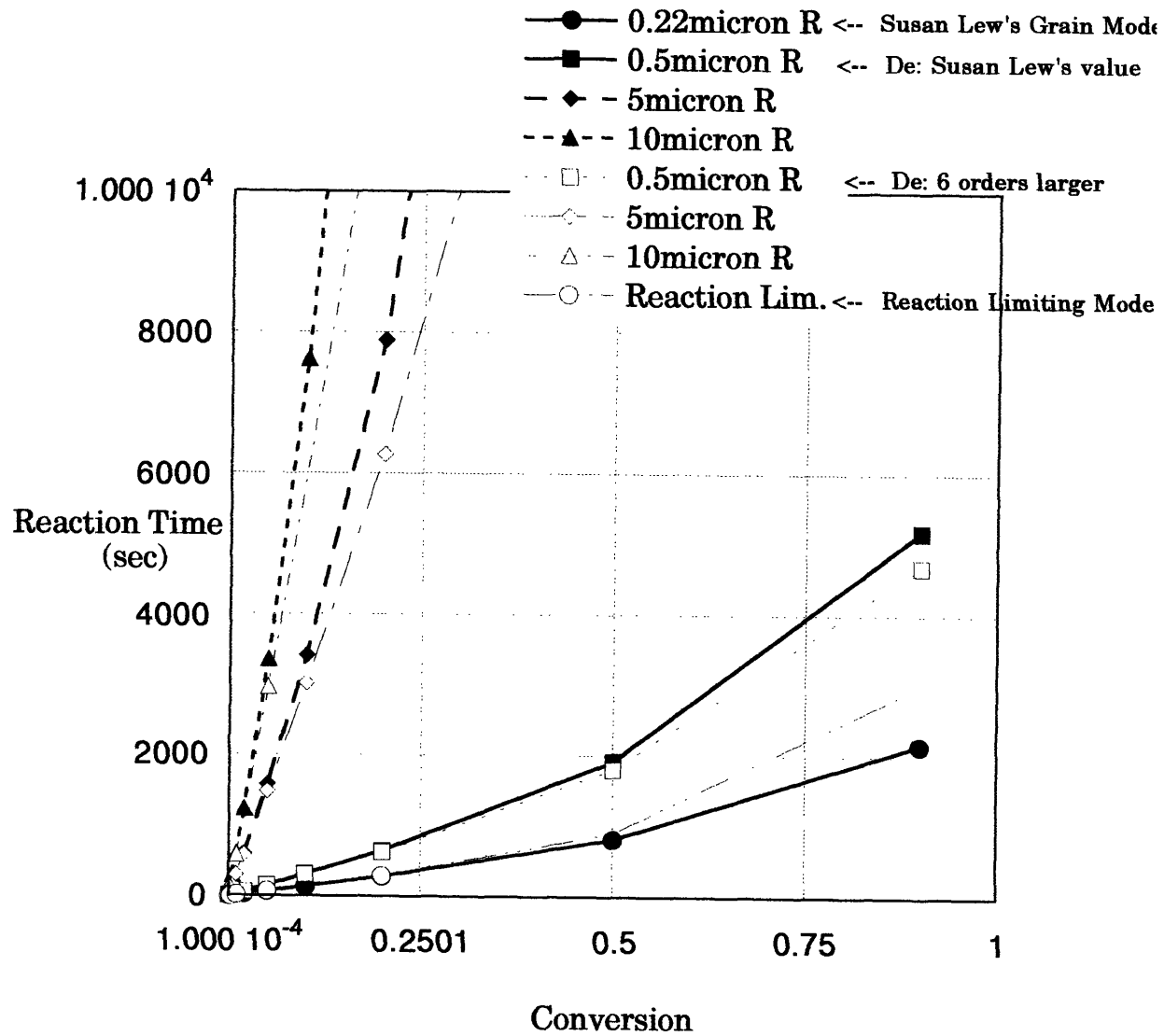


Figure 4.5 Conversion Curves by Reaction Models
(0.4% H₂S, 750 C)

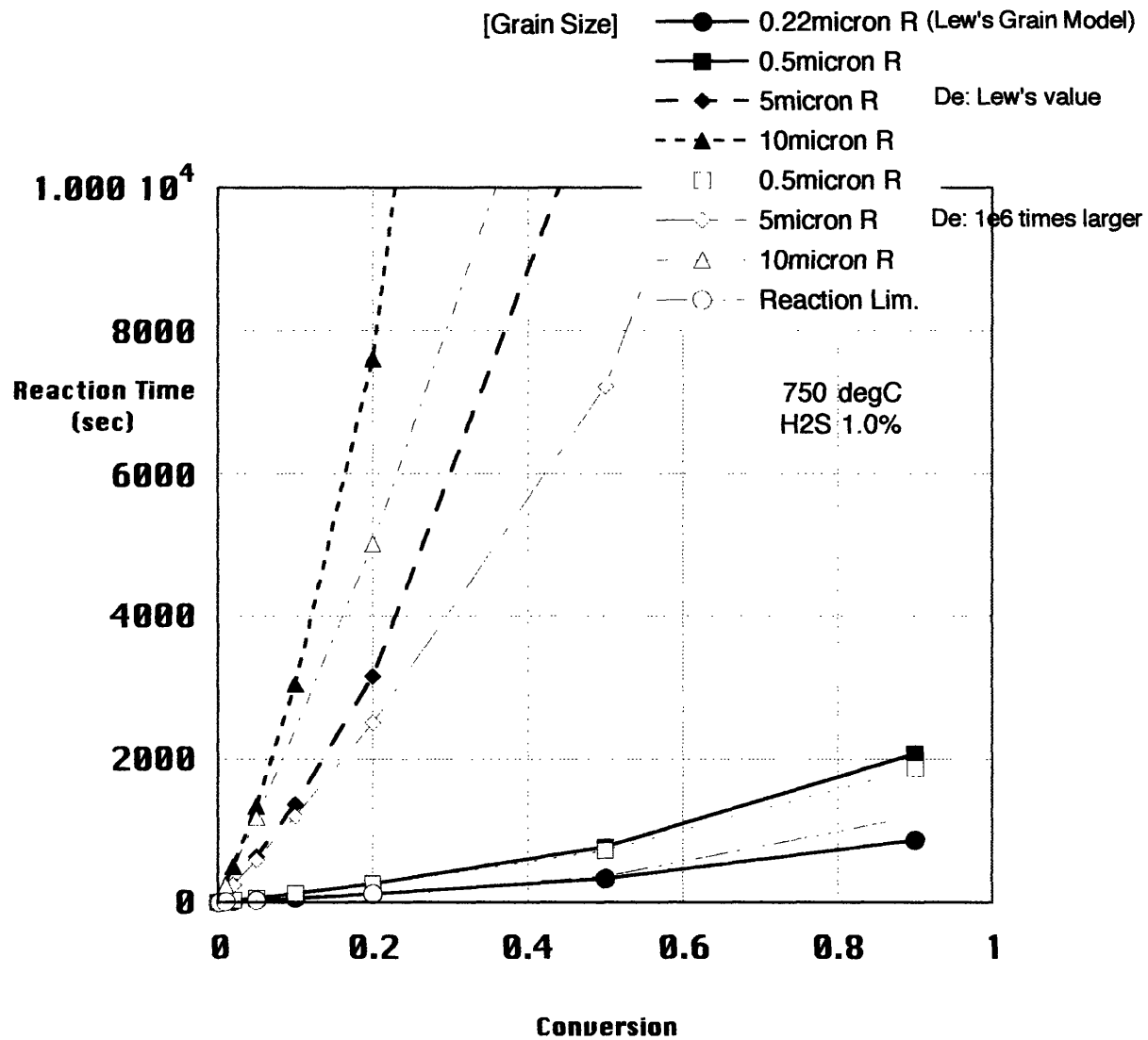


Figure 4.6 Conversion Curves by Reaction Models
(1.0% H₂S, 750 C)

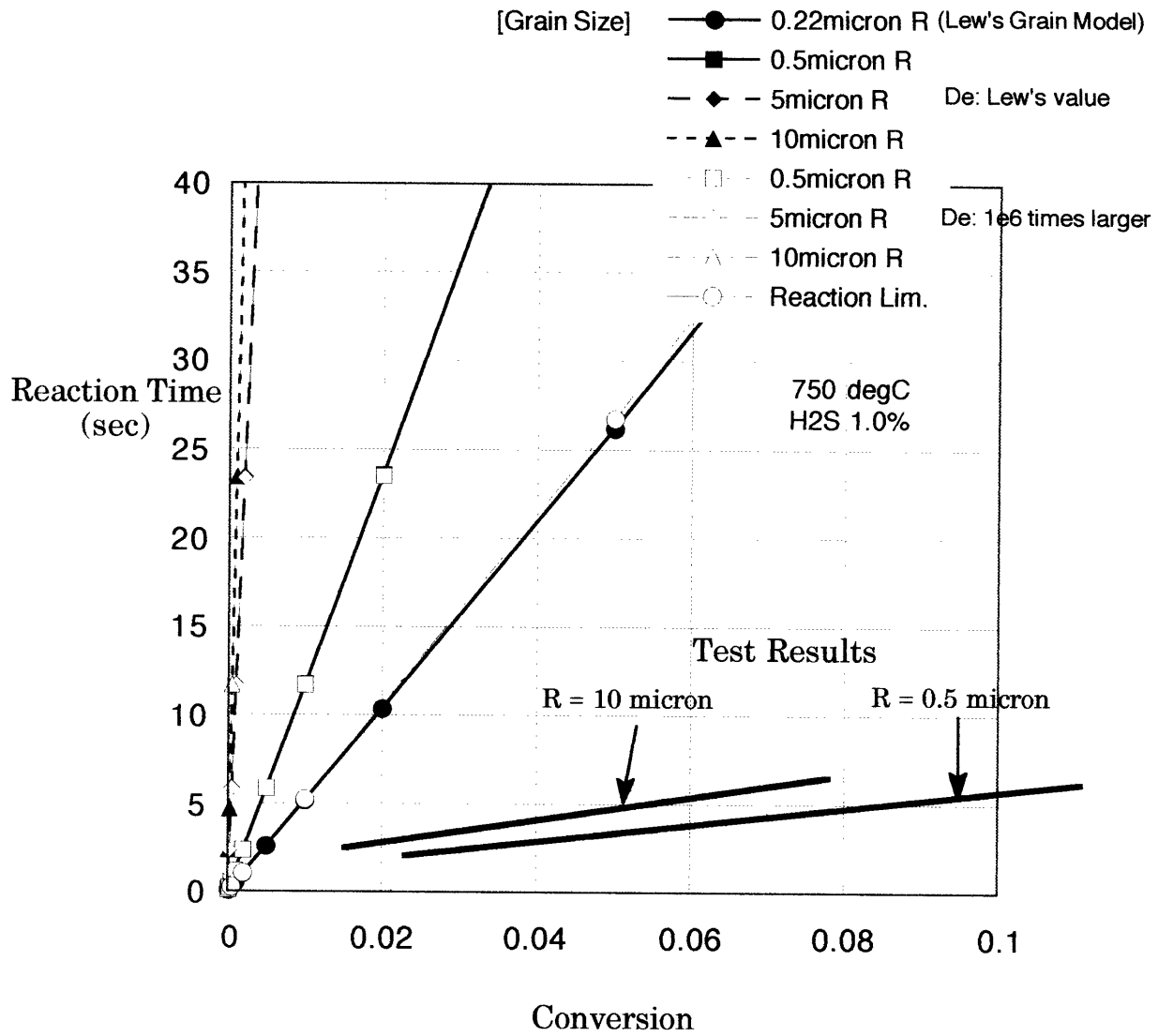


Figure 4.7 Conversion Curves
Test Results vs. Reaction Models
(1.0% H2S, 750 C)

in the drop-tube reactor. However, uniform gas composition and particle velocity at bulk composition and flow rate were assumed here for simplification, that is, H₂S concentration was 1 % and particle velocity was 5 cm/s throughout the reaction region in the case of Figure 4.7.

One significant differences between models and test results is that the experimentally observed conversion was 5 ~ 10 times larger even than the surface reaction limitation model. As shown in the previous section, the mixing model of the drop-tube reactor suggests that the integral of H₂S concentration in the jet flow throughout the reaction region is 46% of the bulk concentration and the retention time of a sorbent particle is 0.3 sec, not that of the bulk flow, 2 sec. If these facts are taken into account, the difference between the models and test results becomes even larger to almost two orders of magnitude. As an example, the conversion of ZnO-2 sorbent with 2 μ m diameter at 750°C in 1%H₂S is predicted by the surface reaction limitation model to be between 0.75% (assuming perfect mixing and 2sec contact time) and 0.05% (assuming the average C_{H₂S} is 46% of C_B and 0.3sec contact time) though the observed conversion was 2.4%. One possible cause of this difference is the enhancement effect of high concentration H₂, but sulfidation conversion even without any H₂ was not much less than other cases. One explanation may be that in the drop-tube furnace, gas phase diffusion resistance is really low and exact surface reaction rate can be measured in comparison with the studies based on TGA.

The particle size dependence of conversion in test results was found to be roughly close to the reaction limitation model based on different surface areas with different sizes and much more moderate than the prediction by the grain model. This indicates that within the range of conversions observed in this study, surface reaction, not diffusion resistance, dominates the overall reaction rate, and that the assumption of each sorbent particle as a non porous grain may not be reasonable. Also, there may be a problem in experiments, that is, variation of retention time among the sorbent particles.

As shown by the mixing model, the jet flow entraining sorbent particles does not transfer completely from turbulent to laminar flow in the reaction region. Therefore, this variation of retention time may make size dependence of conversion unclear. This is also suggested by the fact that in the experiments with longer (30cm) reaction zone, the size dependence of conversion was more apparent than the experiments with 5 or 10 cm reaction zone, although still not so strong as the grain models.

4.5 Conclusions

- 1) The existence of gas composition and particle velocity distribution in the reaction region was found and this was mathematically modeled.

- 2) Two reaction models were examined and compared with test results. It was found that test results showed much higher conversions than models and particle size dependence coinciding with surface reaction limitation model. This shows that the gas phase diffusion resistance is very low in the drop-tube reactor. The reaction models, particularly the value of the initial surface reaction rate should be further modified based on drop-tube experimental results, and some of the experimental conditions, particularly the length of the reaction zone, should also be re-considered.

CHAPTER 5

CONCLUSIONS AND RECOMMENDATIONS

5.1 Conclusions

- 1) At 750°C or lower temperature, H₂S was found to almost completely inhibit the size decrease of sorbent particles caused by vaporization of metallic Zn formed by reduction of ZnO with H₂. This effect seems to be mainly suppression of zinc vaporization, not the reduction reaction.

- 2) At 850°C, fine particles less than 0.3 μm in diameter were formed even in the presence of H₂S. These fine particles were found to be ZnS formed by the reaction of zinc vapor and H₂S and would be possibly captured by micro filtration. Therefore, even at this temperature, vaporization of metallic zinc and formation of fine particles may not be a serious problem in the case of sorbent injection process.

- 3) The effect of reduction reaction enhancing overall sulfidation conversion was observed in these experiments only as 2) above.

- 4) ZnO sorbent has high potential for the sorbent injection hot gas cleanup process.

- 5) Two reaction models were examined and compared with test results. It was found that test results showed much higher conversions than models and particle size dependence coinciding with surface reaction limitation model. This shows that the gas phase diffusion resistance is very low in the drop-tube

reactor. The reaction models, particularly the value of the initial surface reaction rate should be further modified based on drop-tube experimental results, and some of the experimental conditions, particularly the length of the reaction zone, should also be re-considered.

5.2 Recommendations

- 1) A more accurate (and complex) model including both mixing and reaction kinetic factors is needed.
- 2) For the uniformity of temperature, a reaction zone shorter than 10 cm is desirable, while a longer reaction zone is necessary for accurate study of reaction kinetics from the measurement of the particle size dependence of conversion.
- 3) Kinetic experiments with various concentrations of H₂S in the carrier gas and various particle sizes (e.g. < 5 μ m; 40-50 μ m) need to be performed to check the kinetic parameters with these in the literature.
- 4) Study of regeneration characteristic is another key of the process.
- 5) Stable cyclic sulfidation / regeneration performance is an important factor in selecting sorbents, and should be studied in this or a similar test system.

CHAPTER 6

REFERENCES

Flytzani-Stephanopoulos, M., Tamhankar, S. S., Gavalas, G. R., Bagajewicz, M. J., Sharma, P. K. High-Temperature Regenerative Removal of H₂S by Porous Mixed Oxide Sorbents. Preprints of Papers, American Chemical Society, Division of Fuel Energy, 30, 4, 16-25 (1985)

Flytzani-Stephanopoulos, M., Gavalas, G. R., Jothimurugesan, K., Lew, S., Bagajewicz, M. J., Sharma, P. K., Patrick, V. Detailed Studies of Novel Regeneratable Sorbents for High-Temperature Coal-Gas Desulfurization Final Report DE-FC21-85MC221930 (1987)

Hasatani, M., Yuzawa, M., Sugiyama, S., & Wen, C. Y. Reactivity of Fe₂O₃ with H₂S Contained in Low Calorie Syngas. Kagaku Kogaku Ronbunshu, 6, 5, 515 (1980)

Hasatani, M., Yuzawa, M., Ogura, K., & Matsuda, H. Regeneration of Sulfated Iron with Oxygen for High-Temperature Desulfurization Cycle of Low Calorie Syngas. Kagaku Kogaku Ronbunshu, 8, 5, 611 (1982)

Hasatani, M., Matsuda, H., & Kumazawa, K. Regeneration of Iron Sulfide Particle Packed Bed in High-Temperature Desulfurization Cycle of Low Calorie Coal Gasified Gas. Kagaku Kogaku Ronbunshu, 15, 2, 372 (1989)

Ishikawa, K., Kawamata, N., & Kamei, K. Development of a Simultaneous Sulfur and Dust Removal Process for IGCC Power Generation System Proc. of Second International Meet. on Hot Gas Cleanup at Univ. of Surrey (1993)

Lew, S. Ph-D Thesis (MIT) 1992

Lew, S., Sarofim, A.F., F-Stephanopoulos, M. Modeling of the Sulfidation of Zinc-Titanium Oxide Sorbents with Hydrogen Sulfide AICHE J. Vol.38, No.8, pp.1161 (1992)

Lew, S., Sarofim, A.F., F-Stephanopoulos, M. The Reduction of Zinc Titanate and Zinc Oxide Solids Chem.Eng.Sci. Vol.47, No.6 pp.1421 (1992)

Lew, S., Sarofim, A.F., F-Stephanopoulos, M. Sulfidation of Zinc Titanate and Zinc Oxide Solids Ind.Eng.Chem.Res. Vol.31, No.8 pp.1890 (1992)

Steinfeld, G. (1982). Hot-Gas Desulfurization. DOE/MC/16545-T1

U.S.DOE (1993) Proc. of the Coal-Fired Power Systems 93 Advances in IGCC and PFBC Review Meet.

Westmoreland, P.R., Gibson, J.B., Harrison, D.P. Comparative Kinetics of High-Temperature Reaction Between H₂S and Selected Metal Oxides. Environ. Sci. Technol. Vol. 11, pp. 488-491 (1977)